Coherent quantum phenomena in ultimate 2D superconductors: A STM study

Dimitri Roditchev

New:

COST Action CA16218

NANOSCALE COHERENT HYBRID DEVICES FOR SUPERCONDUCTING QUANTUM TECHNOLOGIES

H. Suderow (UAM, Spain)

http://www.cost.eu/COST_Actions/ca/CA16218

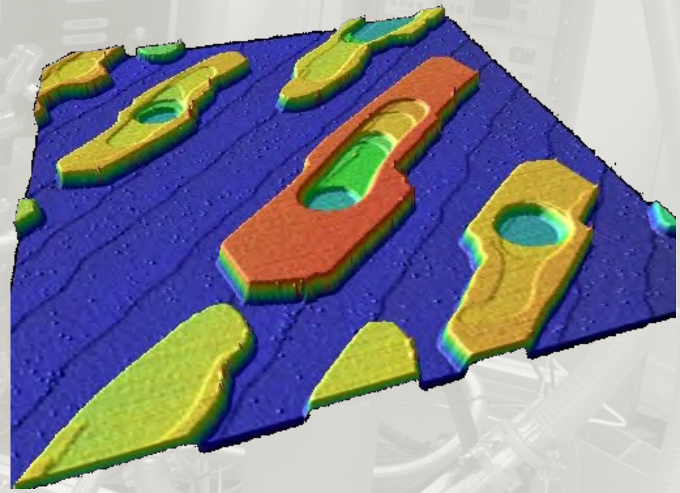

SPICE, Mainz, Sept. 25th–28th 2017

Coherent quantum phenomena in ultimate 2D superconductors: A STM study

Dimitri Roditchev

Tristan **Cren**
Christophe **Brun**
Lise **Serrier-Garcia** (KU Leuven)
Vladimir Cerchez (CEA, Saclay)
Denis Fokin (ISSP, Chernogolovka)
Vasily Stolyarov (MIPT, Dolgoprudny)
François Debontridder
Stéphane Pons
Gerbold **Ménard** (PhD 2014-2016)

Juan-Carlos Cuevas (IFIMAC, Madrid, Spain)
Milorad Milosevic and coll. (Antwerpen Univ.)
Lev Ioffe (Rutgers and Paris 6 Univ.)
Boris Altshuler (Columbia Univ.)
Michael Tringides (Iowa State Univ.)
Sergey Bozhko (ISSP, Chernogolovka)
Pascal Simon (LPS, Orsay, France)

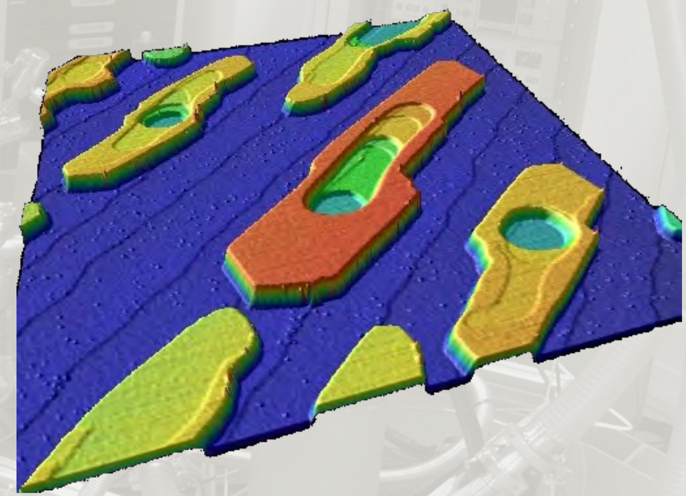

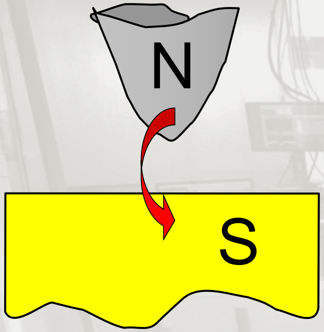

Scanning Tunneling Spectroscopy

$$\frac{dI}{dV}(V) = -\frac{2\pi e^2 T}{\hbar} N_p \int_{-\infty}^{\infty} N_S(E+eV)\ \frac{\partial f}{\partial E}(E)\,dE$$

Visualization of the vortex cores at the ***Gap Edge***

Hess et al. (1989)

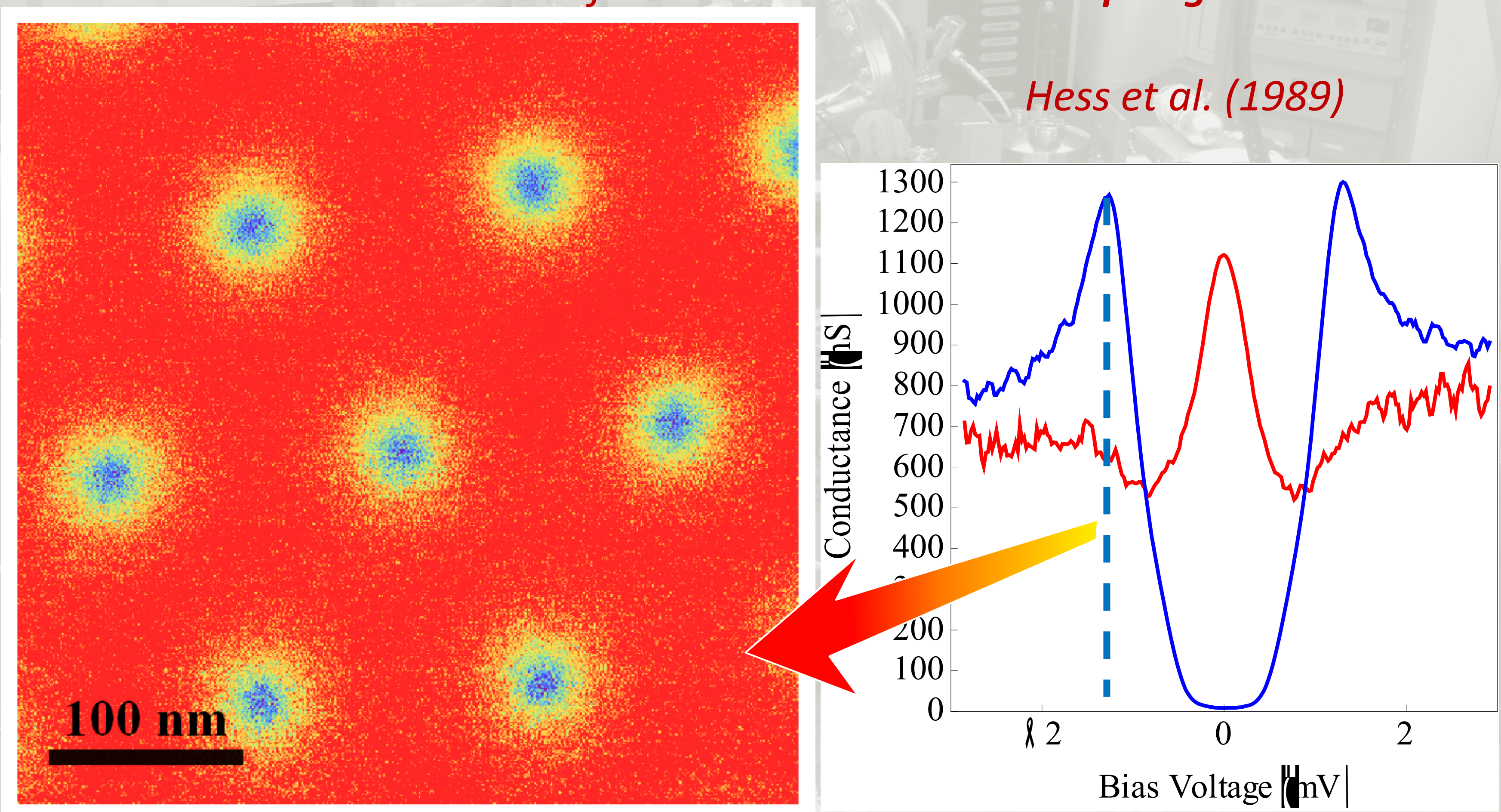

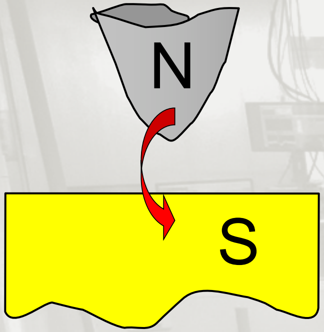

Scanning Tunneling Spectroscopy

$$\frac{dI}{dV}(V) = -\frac{2\pi e^2 T}{\hbar} N_p \int_{-\infty}^{\infty} N_S(E+eV)\ \frac{\partial f}{\partial E}(E)dE$$

Visualization of the vortex cores at ***Zero Bias***

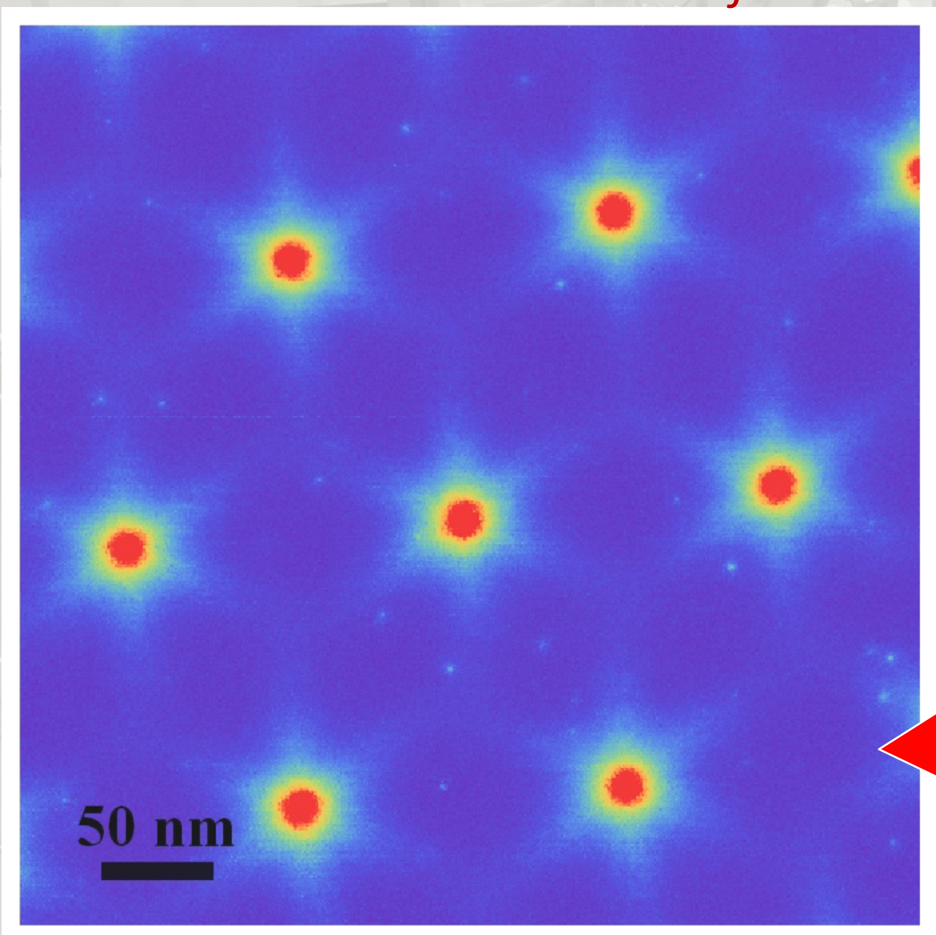

Hess et al. (1989)

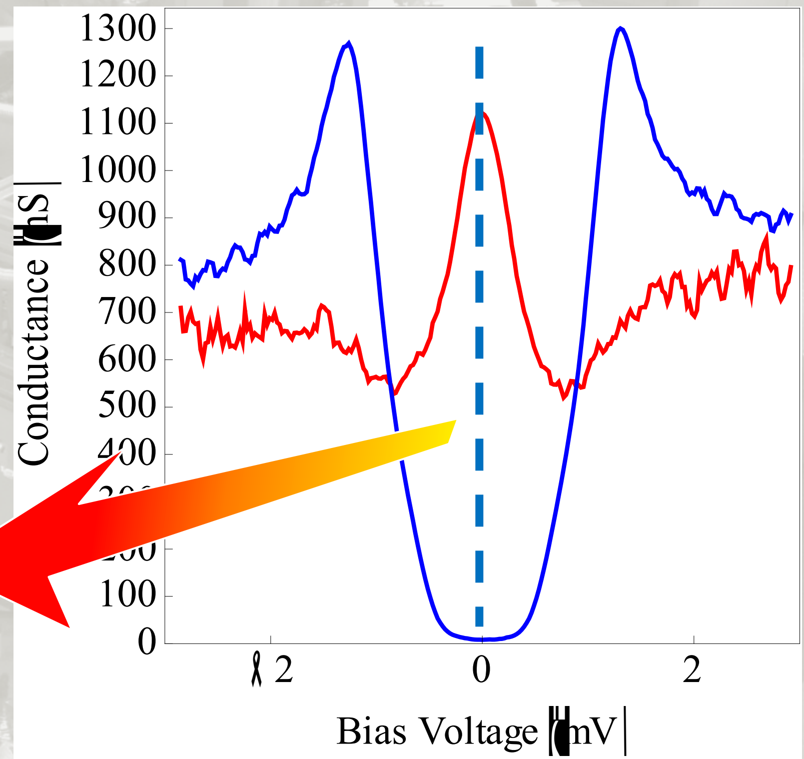

Inter-vortex distance = 49.8nm@1T – STM scanner calibration

Outlook

Elementary excitations and vortex in superconducting **Pb-monolayers** *Nat. Phys. (2014)*

Josephson vortex matter in **proximity** junctions *PRL (2013), PRX (2014), Nat. Phys. (2015)*

Long-range Shiba bound states in 2D limit *Nat. Phys. (2015)*

Unconventional **collective** bound states *(2017) to be published*

Pb growth on 7x7 Si(111) in UHV

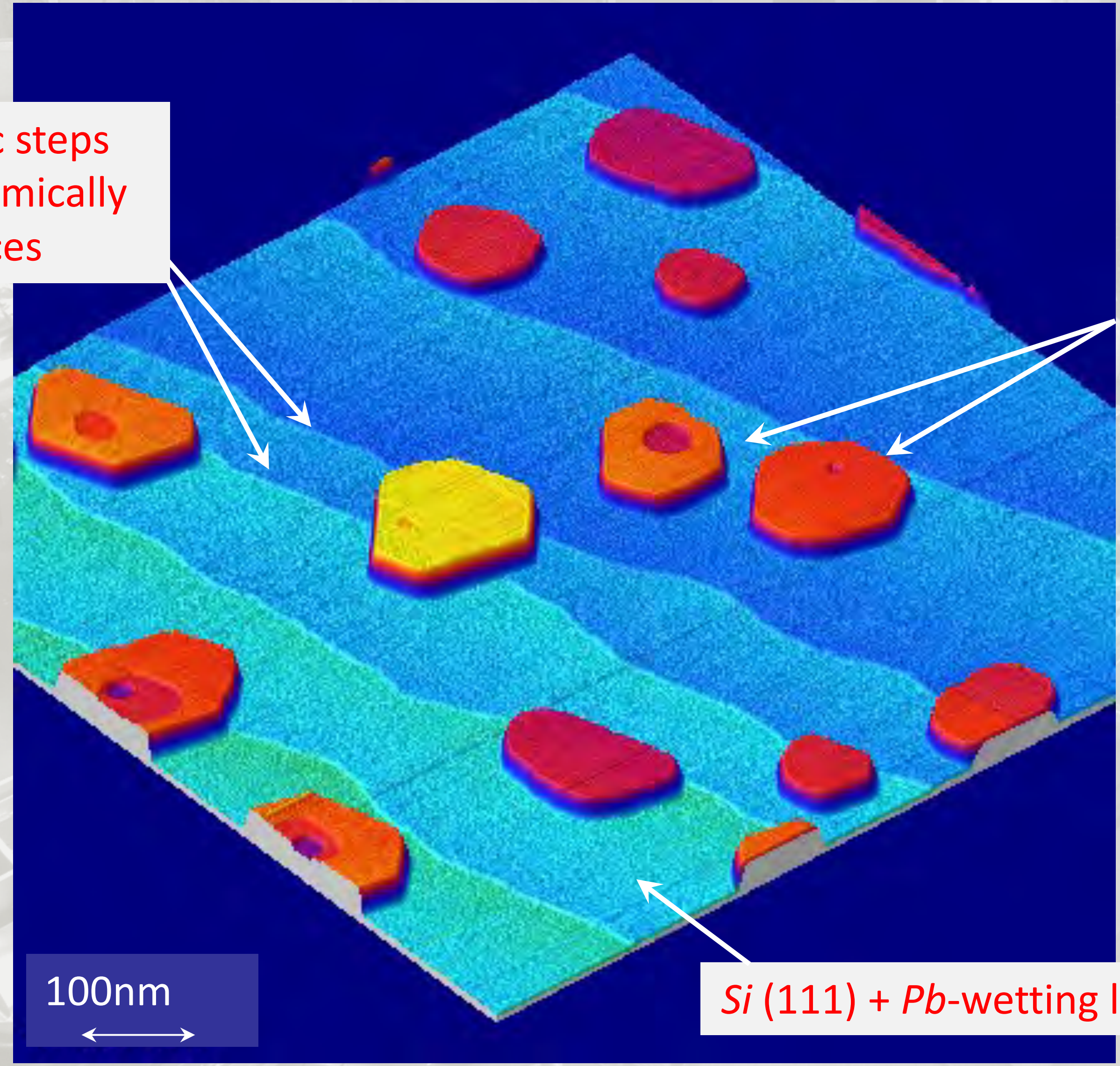

Pb growth on 7x7 Si(111) in UHV

7x7 Si(111)

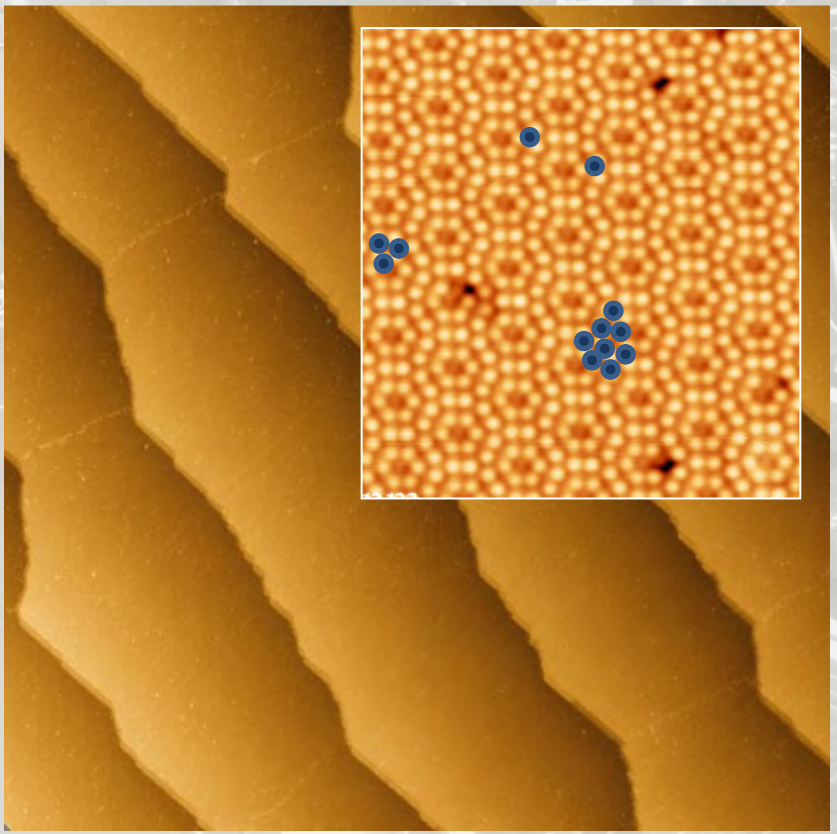

100nm

What is important:

- Pressure (vacuum)
- Temperature
- Source cleanness
-Evaporation rate
- Evaporated amount
- Post-treatment

L. Serrier-Garcia et al, J. Phys. Chem. C 119, 22 12651-12659 (2015)

Pb growth on 7x7 Si(111) in UHV

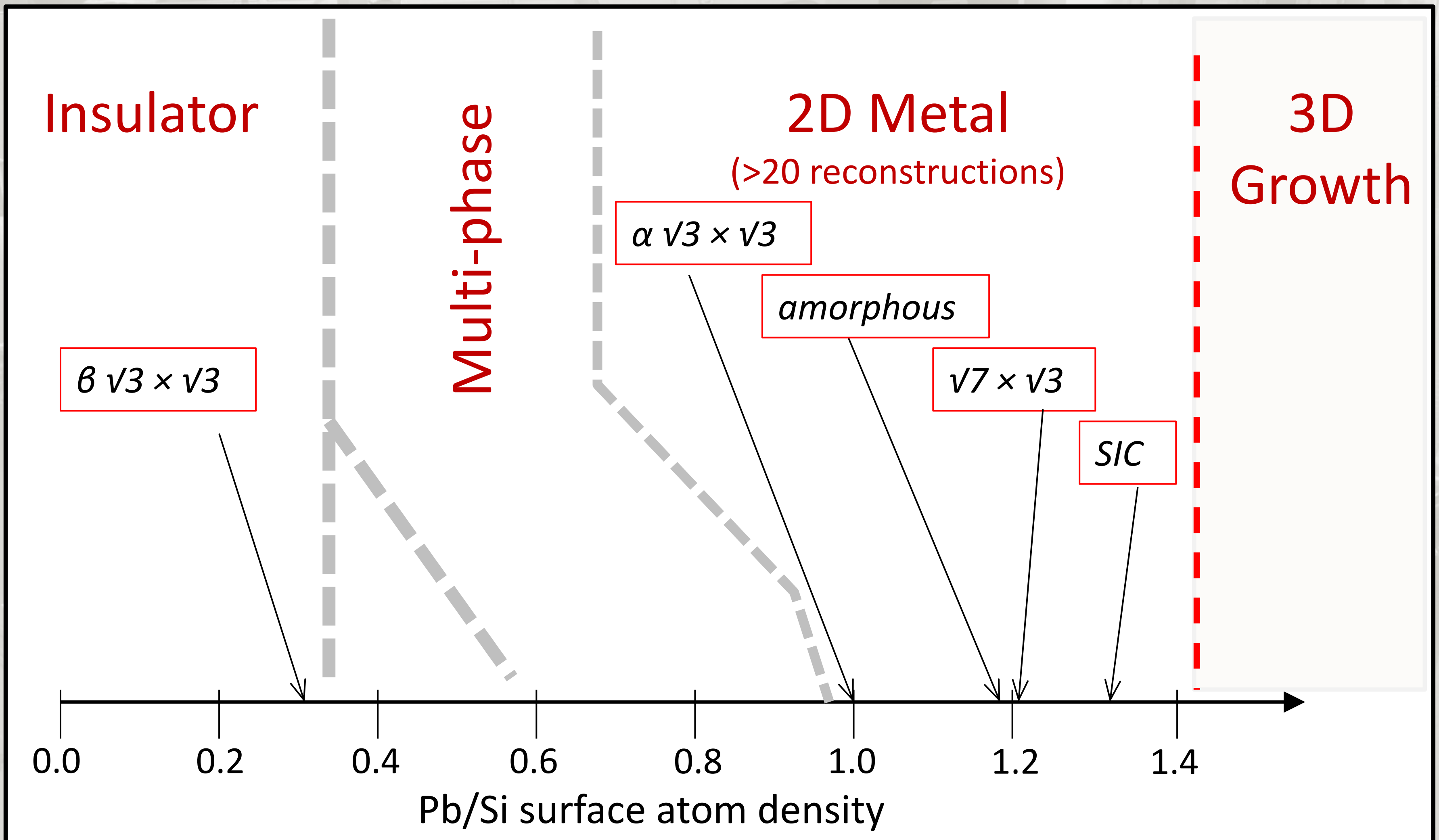

Pb growth on 7x7 Si(111) in UHV

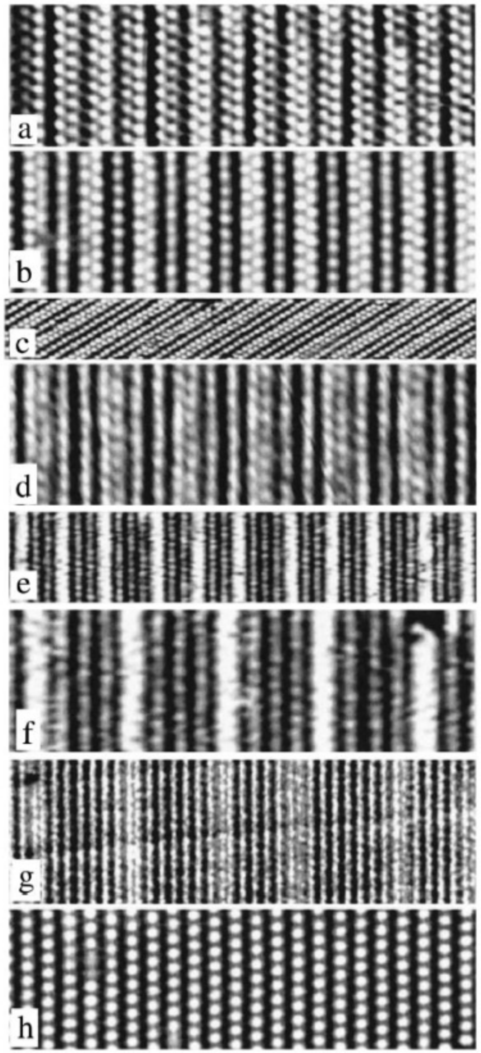

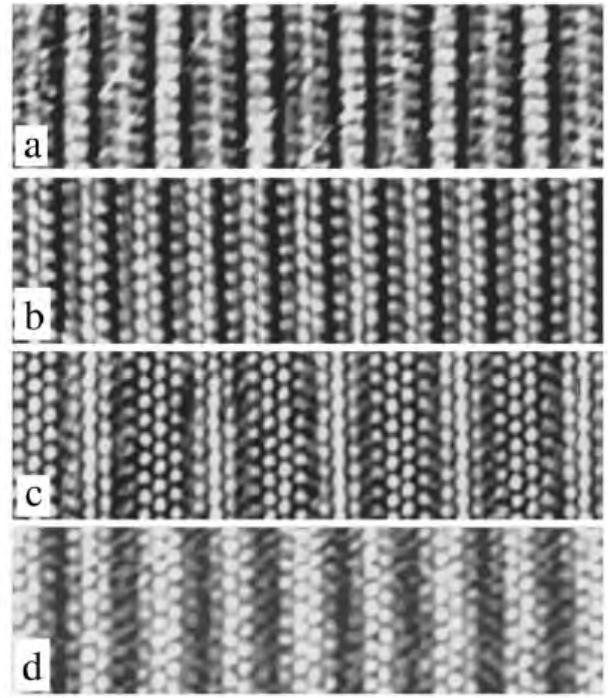

FIG. 3. Linear phases in the range $1.25 < \beta < 1.3$ ML: (a) $n = 1, m = 1$ and 2 $\beta = 1.263$ ML; (b) $n = 1, m = 2$ $\theta = 1.27$ ML; (c) $n = 1, m = 3$ and 2 $\theta = 1.28$ ML; (d) $n = 1, m = 3$ $\theta = 1.285$ ML.

M. Hupalo, J. Schmalian, and M. C. Tringides, Phys. Rev. Lett. (2003)

Superconductivity in atomically thin Pb/Si(111)

Discovery

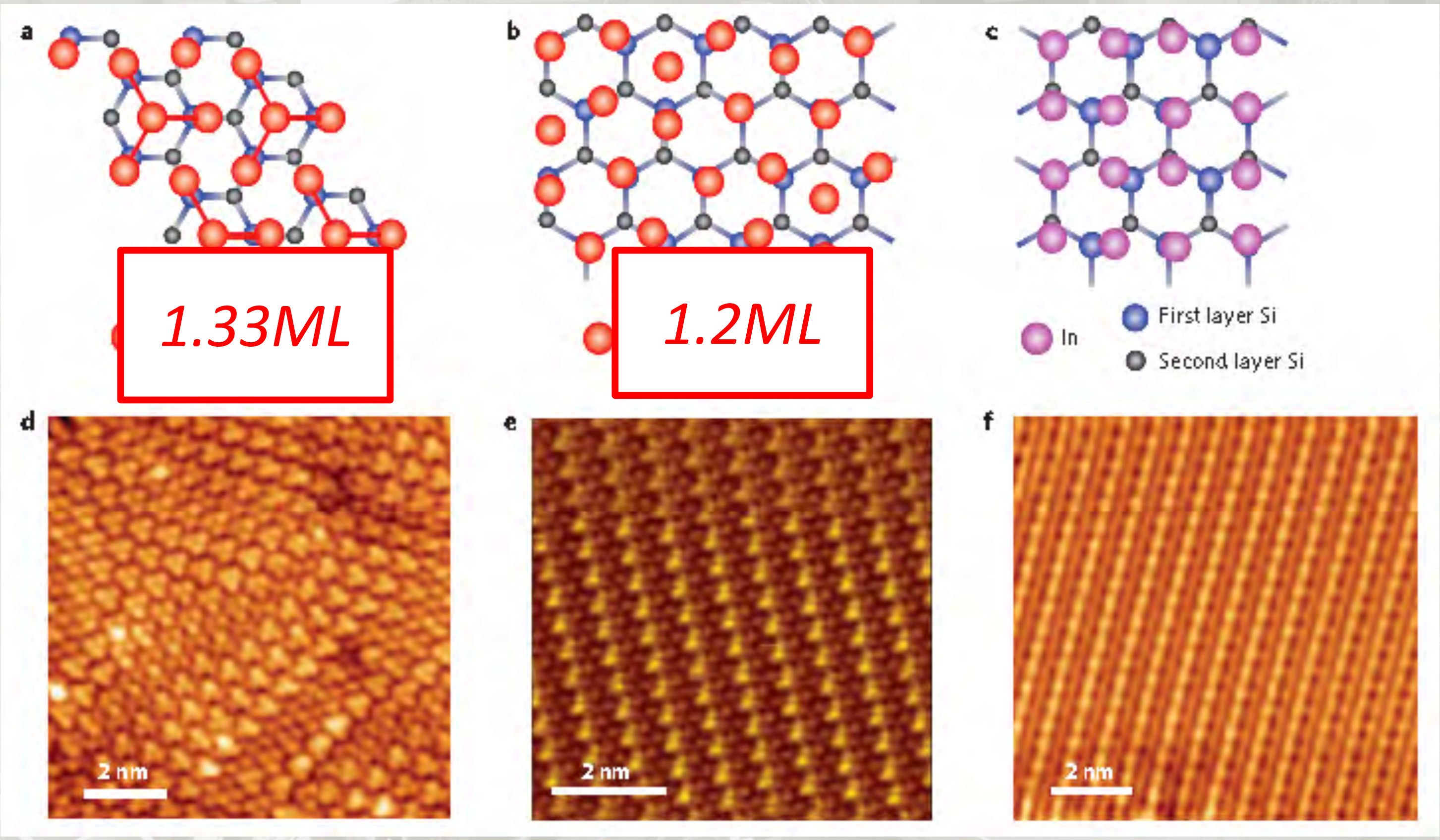

SIC-Pb *√7 × √3-Pb* *√7 × √3-In*

S. Zhang et al. Nature Phys. 6, 104 (2010)

Superconductivity in atomically thin Pb/Si(111)

Pb growth on 7x7 Si(111) in UHV

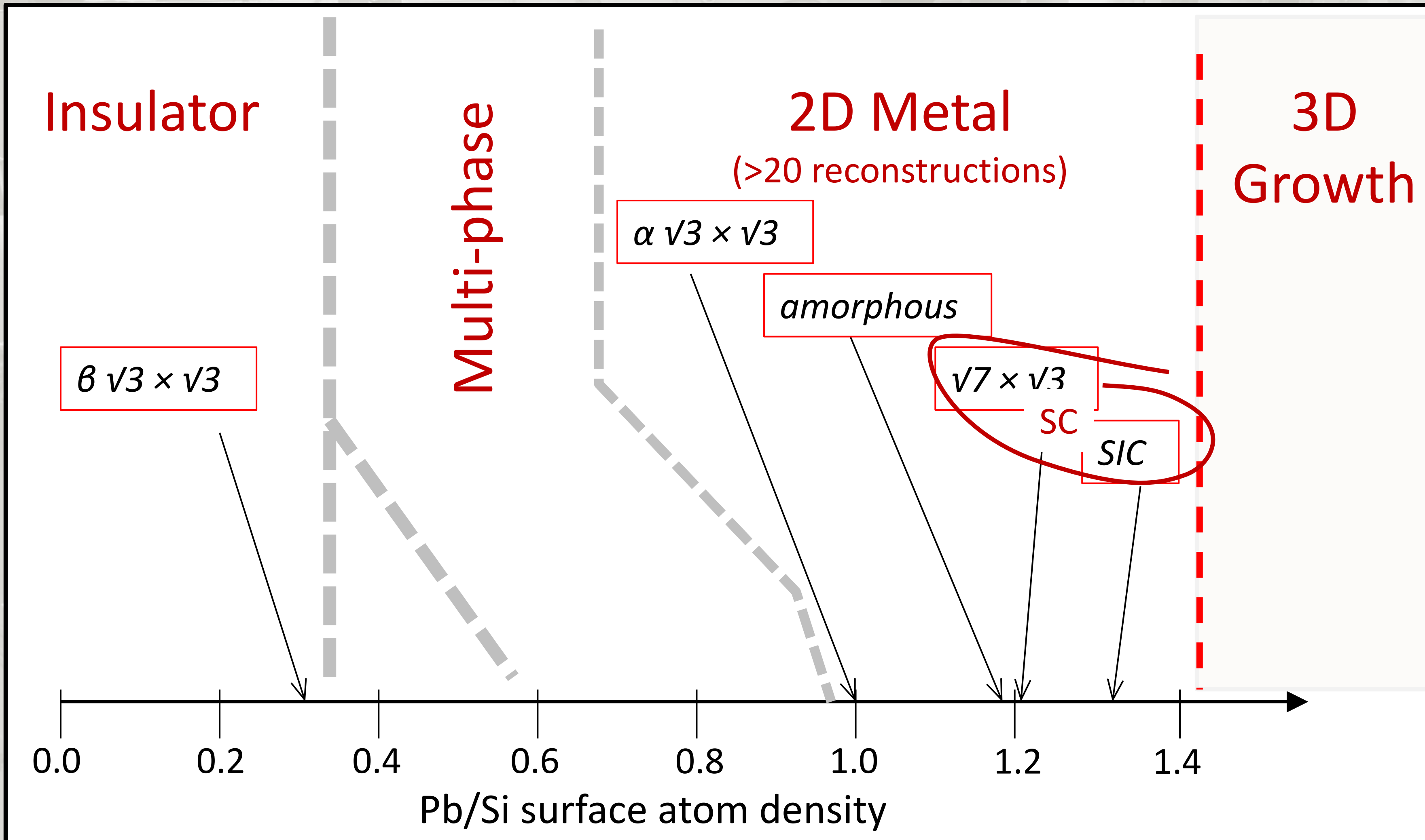

Superconductivity in atomically thin Pb/Si(111)

Influence of atomic disorder on the LDOS

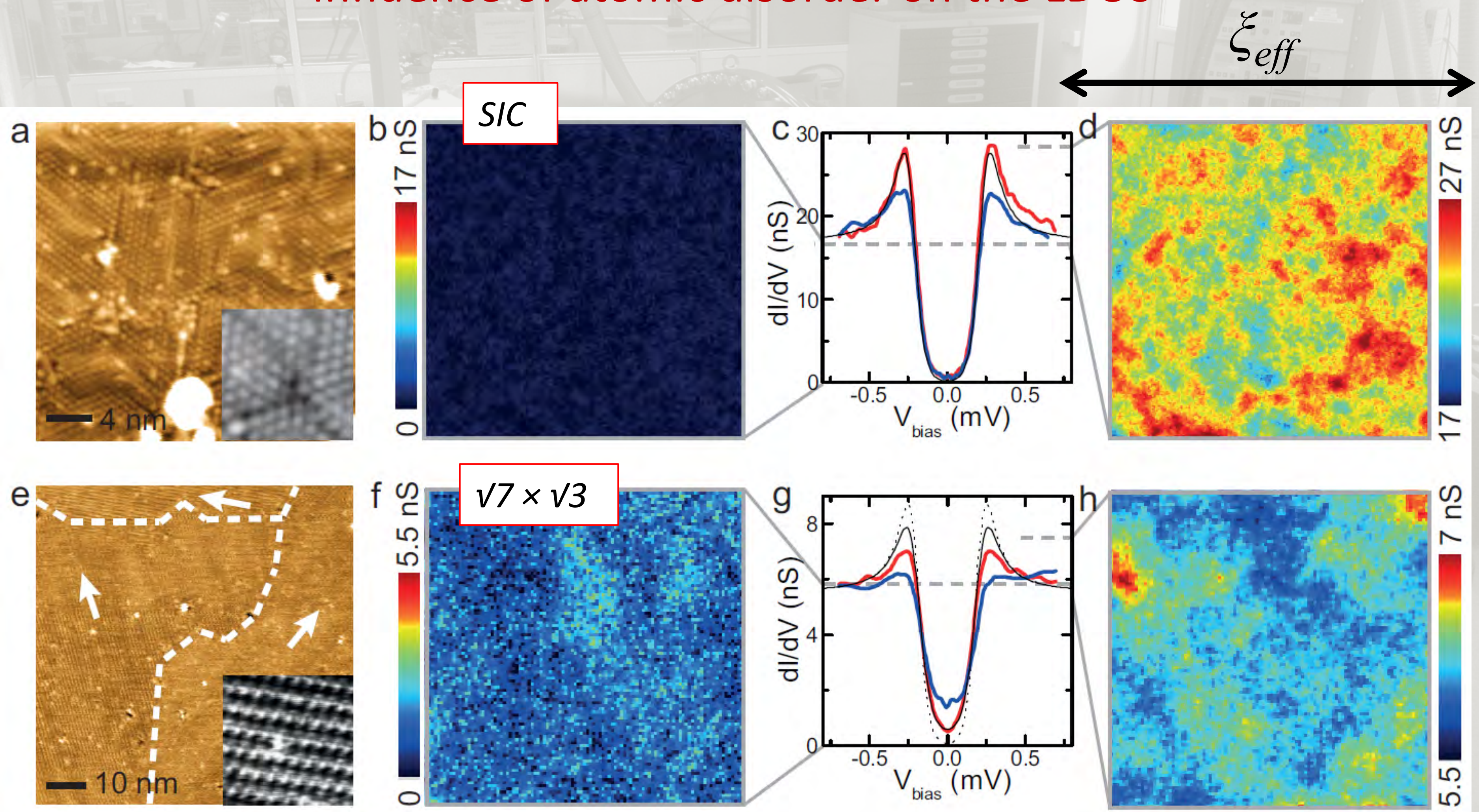

C. Brun et al. Nat. Phys. 10, 444 (2014)

Superconductivity in atomically thin Pb/Si(111)

Step structure

√7 × √3

√7x √3 Pb step (atomic resolution)

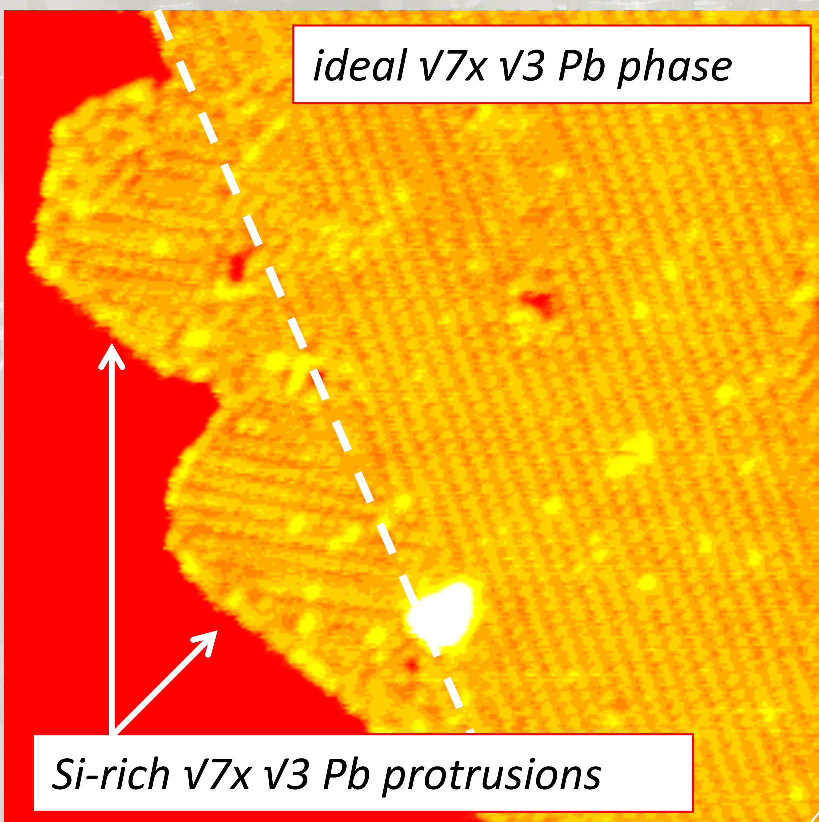

√7x √3 Pb / Si(111)

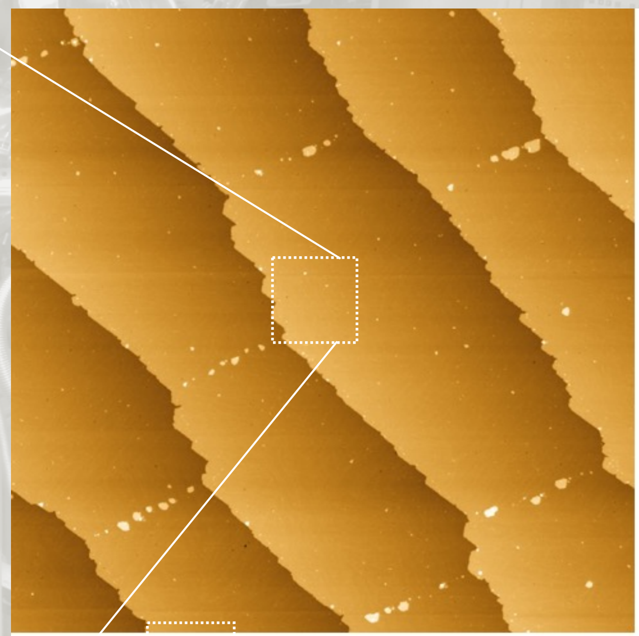

C. Brun et al. Nat. Phys. 10, 444 (2014)

Superconductivity in atomically thin Pb/Si(111)

SC Gap near atomic steps

SIC

√7 × √3

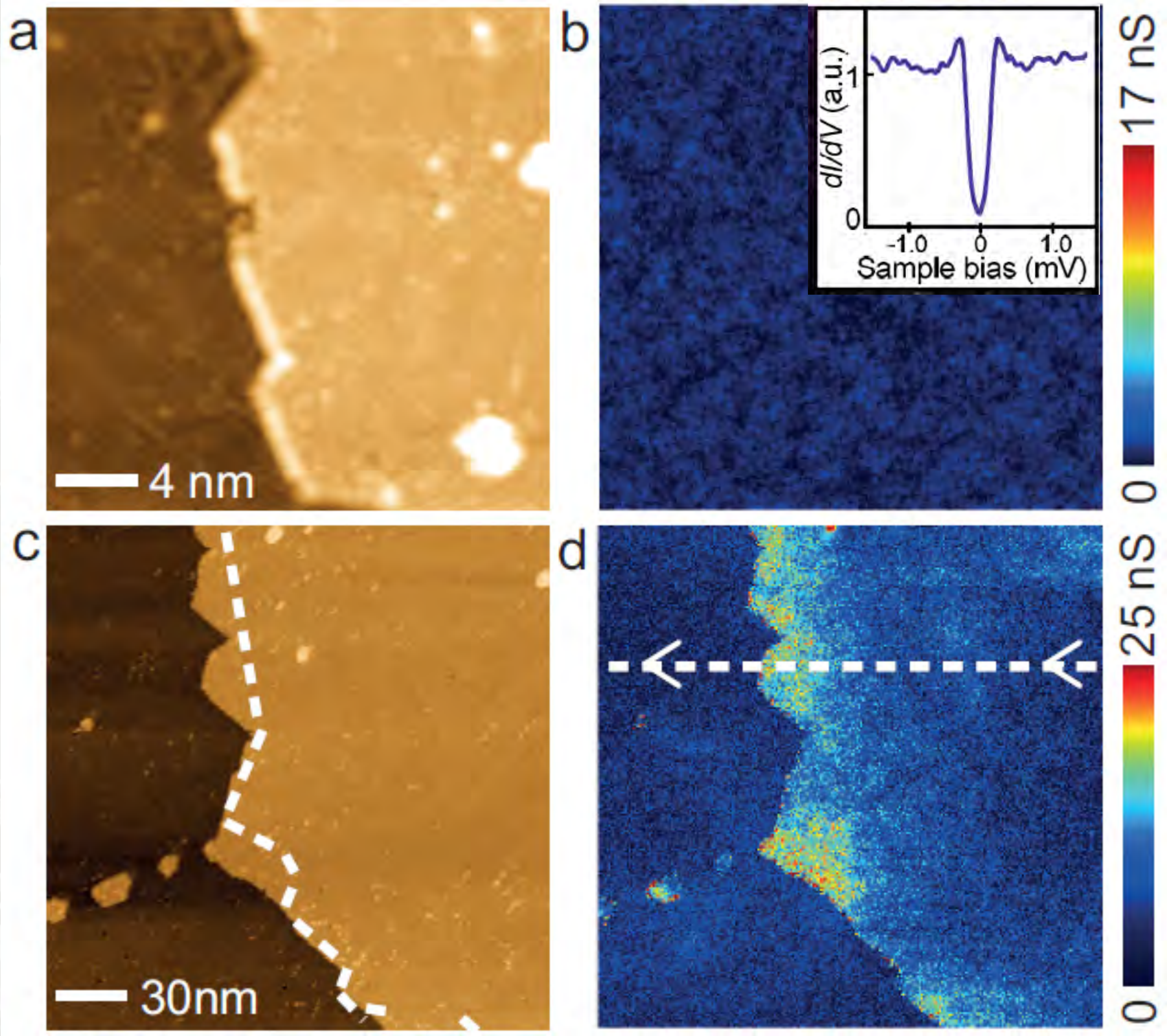

C. Brun et al. Nat. Phys. 10, 444 (2014)

Superconductivity in atomically thin Pb/Si(111)

SC Gap near atomic steps

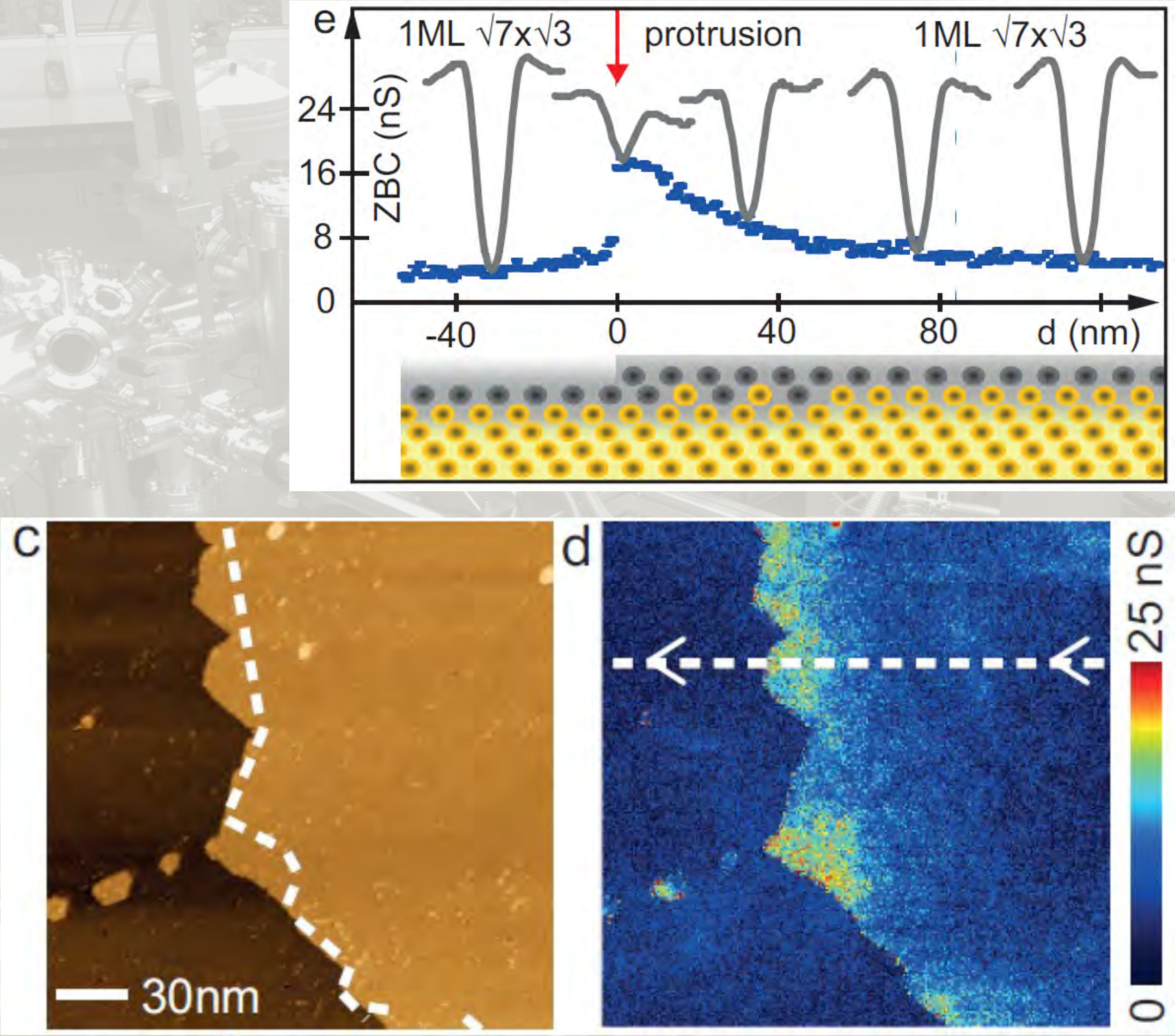

√7 × √3

C. Brun et al. Nat. Phys. 10, 444 (2014)

Superconductivity in atomically thin Pb/Si(111)

SC Gap near atomic steps

√7 × √3

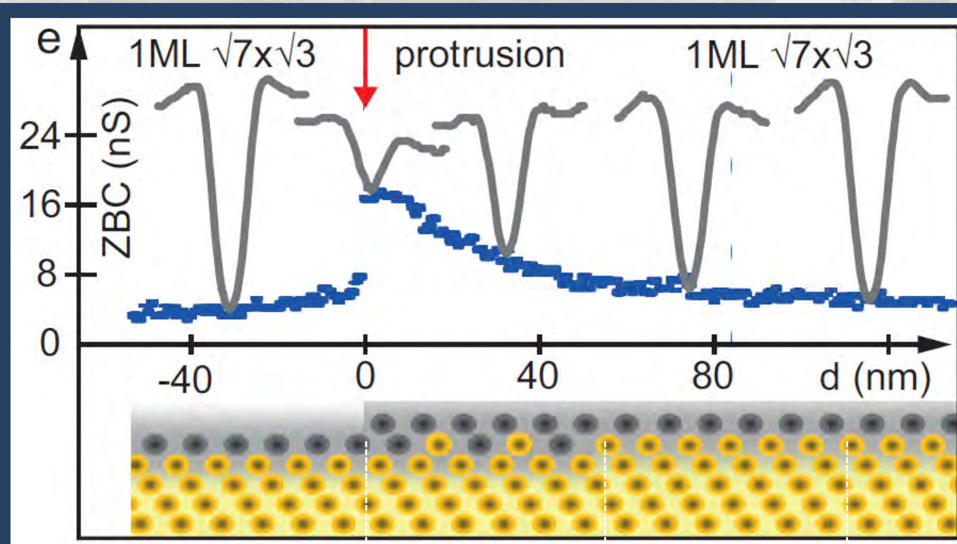

Sharp Josephson barrier

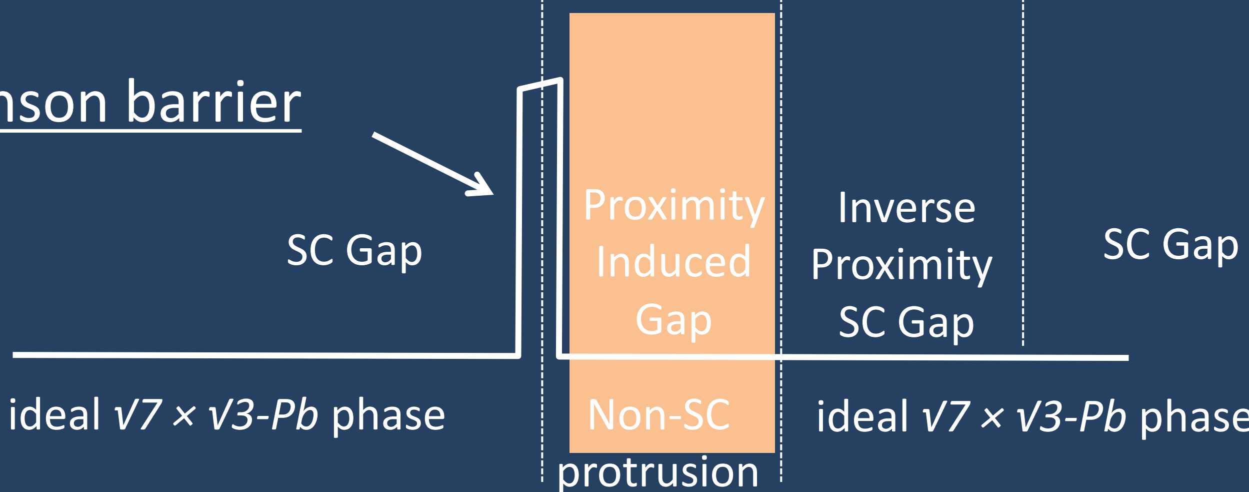

C. Brun et al. Nat. Phys. 10, 444 (2014)

Superconductivity in atomically thin Pb/Si(111)

Vortex matter in √7 × √3-Pb

√7 × √3

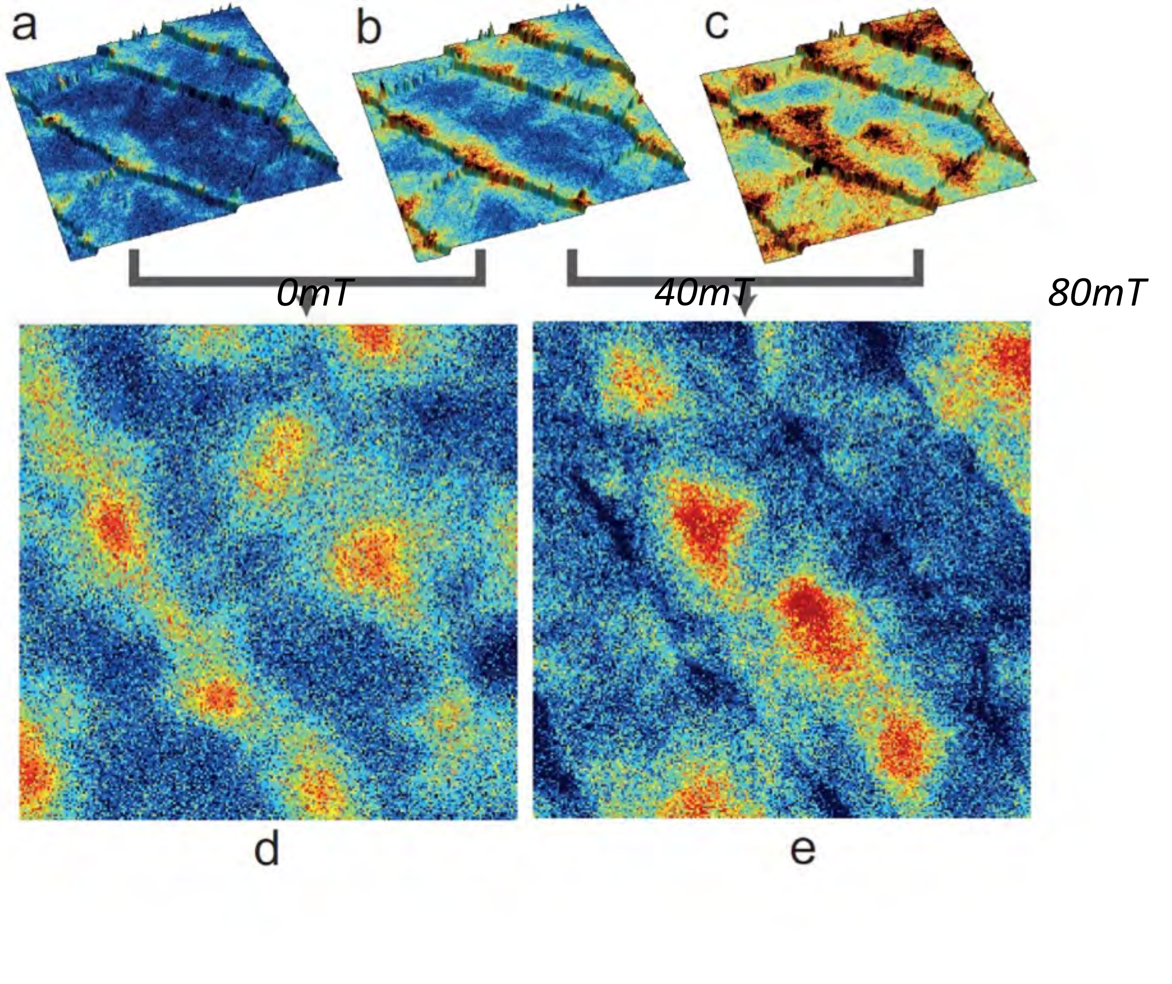

Tc=1.5K

T_{STS}=0.3K

At B<40 mT the vorex cores appear small; they are all pinned at steps
At B>80 mT new vortices appear on *terraces*

C. Brun et al. Nat. Phys. 10, 444 (2014)

Superconductivity in atomically thin Pb/Si(111)

Abrikosov-Josephson vortex in √7 × √3-Pb

Abrikosov-Josephson vortex *(A. Gurevich, 1993)*

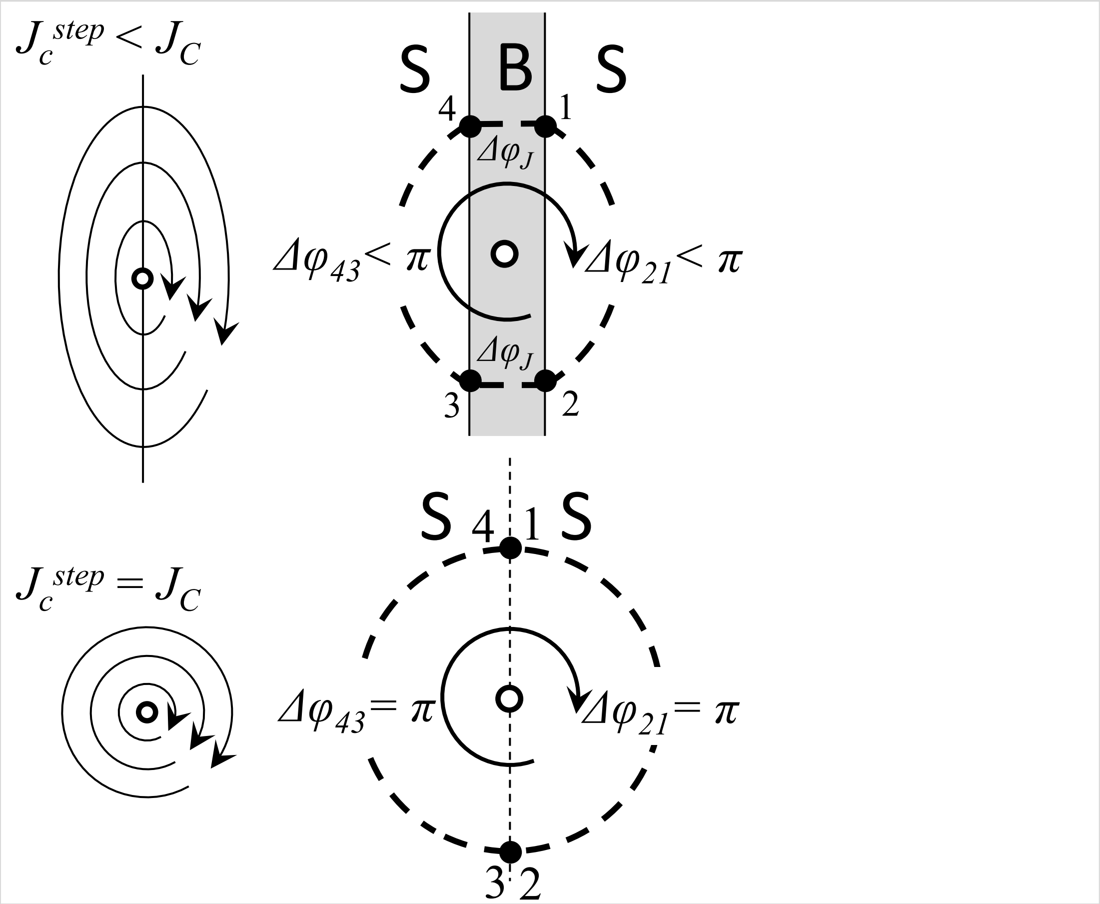

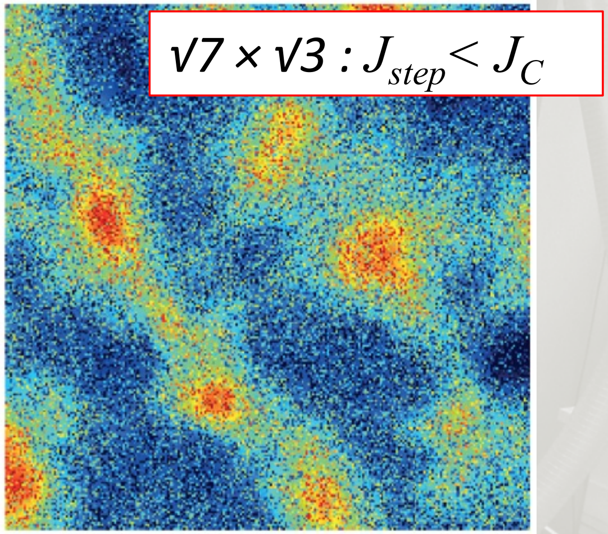

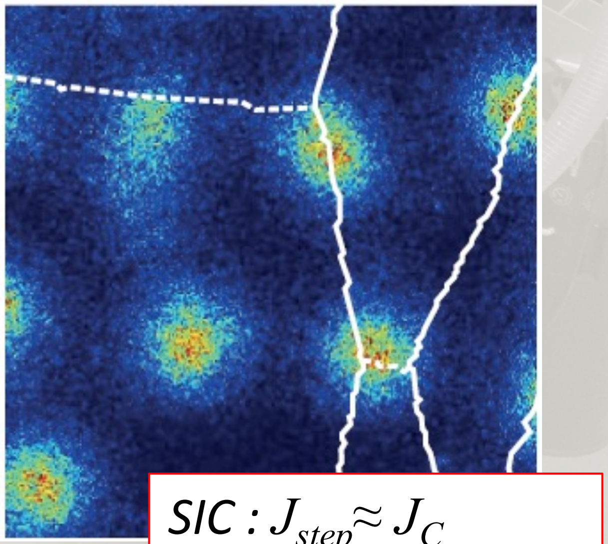

C. Brun et al. Nature Phys.(2014)

Superconductivity in atomically thin Pb/Si(111)

Abrikosov-Josephson vortex in √7 × √3-In

Abrikosov-Josephson vortex *(A. Gurevich, 1993)*

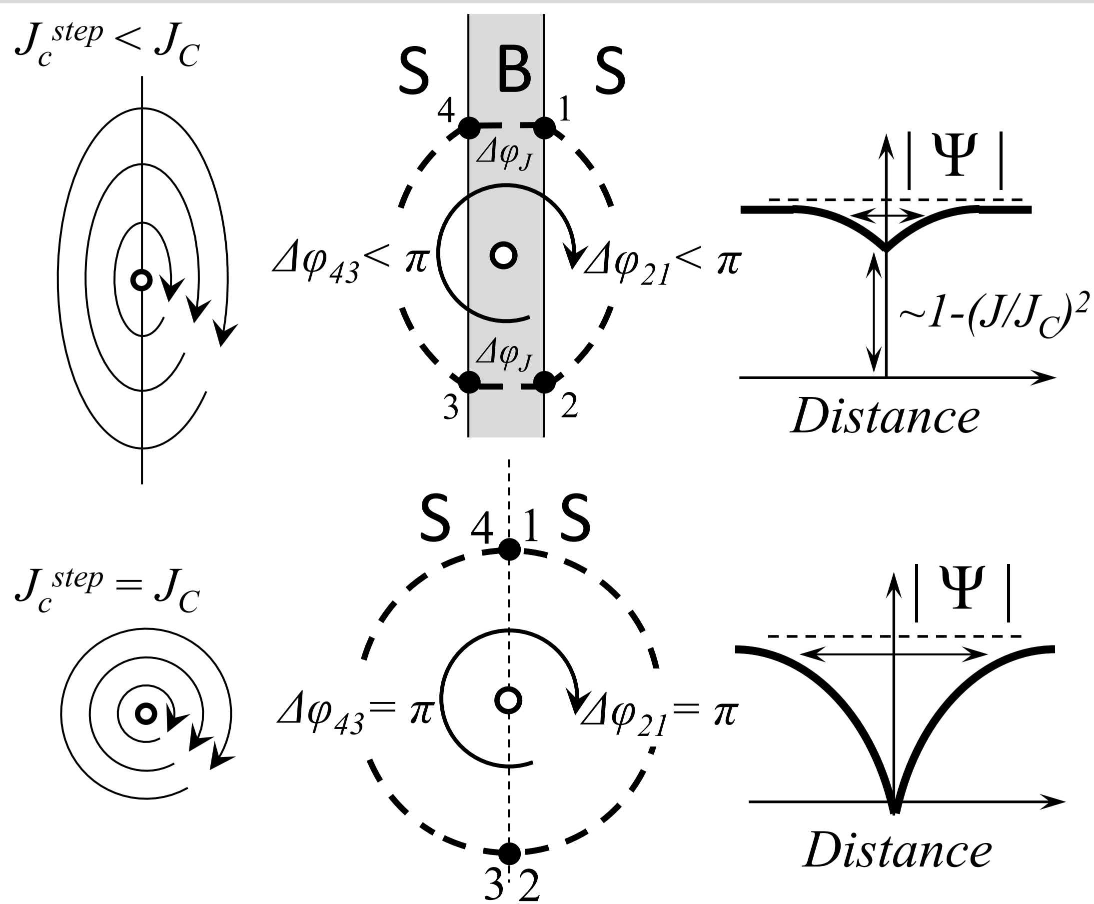

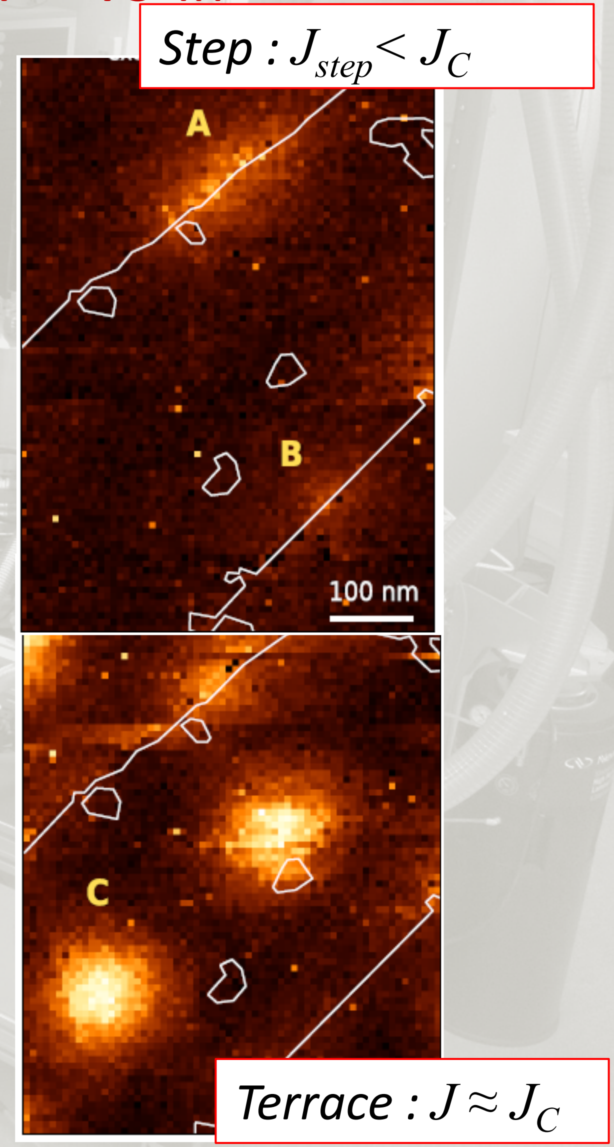

S. Yoshizawa et al. Phys. Rev. Lett.(2014)

Conclusions 1/4

Amorphous Pb/SI(111) is not SC down to 300mK

Among > 20 reported Pb/Si(111) crystalline phases only SIC and √7 × √3 were studied and found SC

Below Tc≈1.5-1.8K both SIC and √7 × √3 layers are phase coherent at least on a mesoscopic scale – they are "real" superconductors

The SC wavefunction is localized at Pb/Si interface within 2-3 atomic layers

√7 × √3 : Atomic steps are native Josephson junctions linking SC terraces

√7 × √3 : Vortex phase: Abrikosov-Josephson vortices are revealed at steps

<u>Remaining questions</u>:

Why is it SC? What is the origin of short range DOS variations? That of the Gap filling in √7 × √3 ?

Outlook

Elementary excitations and vortex in superconducting **Pb-monolayers** — *Nat. Phys. (2014)*

Josephson vortex matter in **proximity** junctions — *PRL (2013), PRX (2014), Nat. Phys. (2015)*

Long-range Shiba bound states in 2D limit — *Nat. Phys. (2015)*

Unconventional **collective** bound states — *(2017) to be published*

Josephson vortex matter in lateral proximity junctions

Pb growth on 7x7 Si(111) in UHV

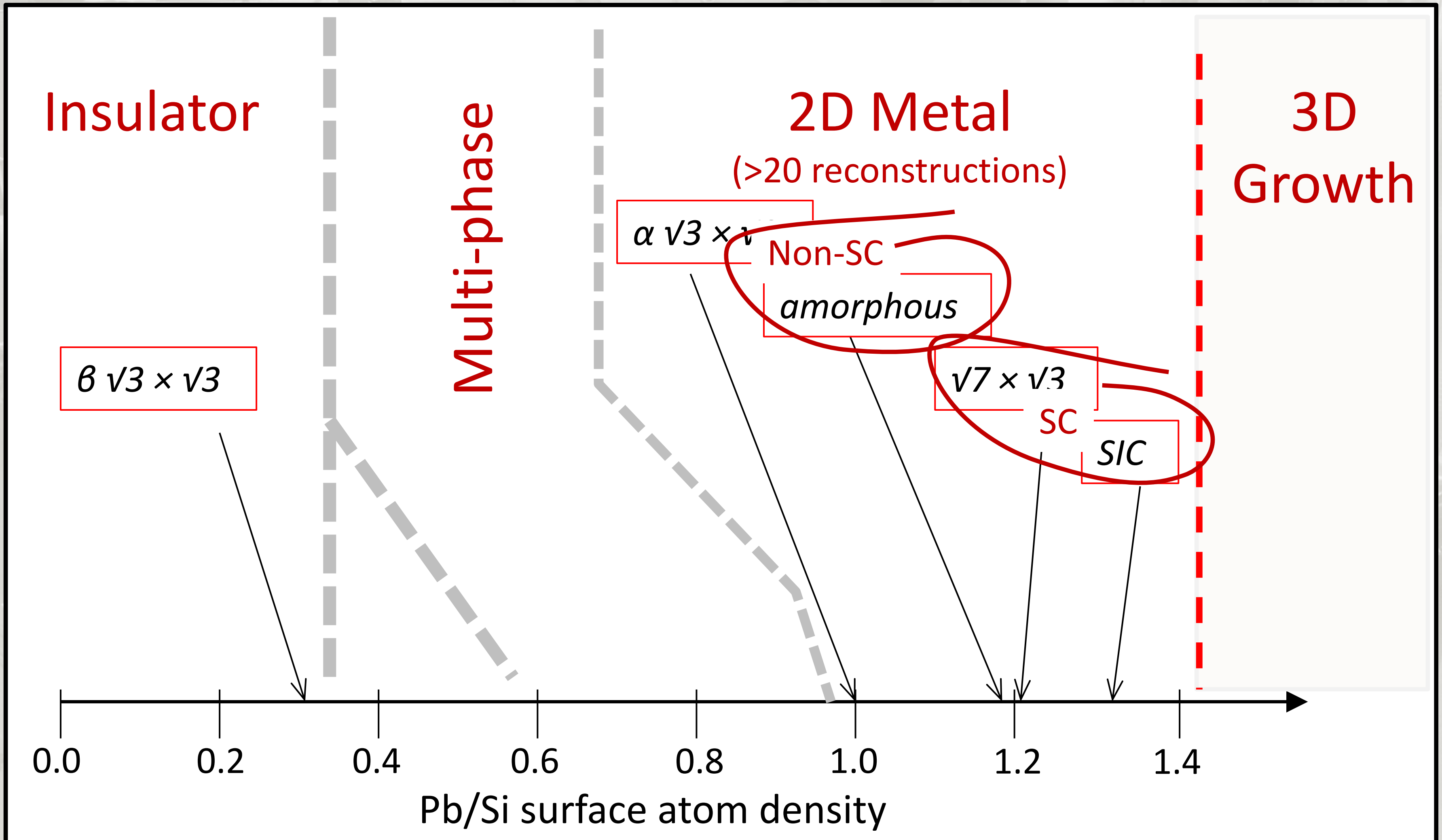

2/4 Josephson vortex matter in lateral proximity junctions

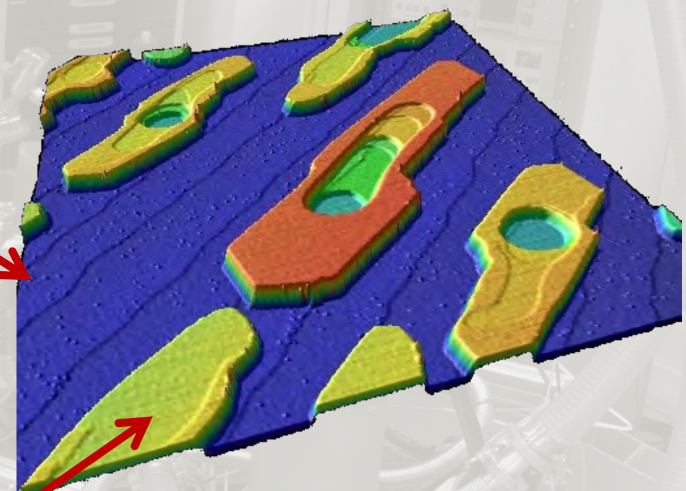

The wetting layer could be made:

- fully **non-superconducting**, $T_C \approx 0$ K

or

-**superconducting** at $T_C \approx 1.5\text{-}2$ K

The islands are SC at $T_C \approx 6.2$K.

Possibility to realize atomically sharp S-N and S-S' interfaces

(PRL 2013, Phys. Rev. X, 2014)

Josephson vortex matter in lateral proximity junctions

2.1. S-S': Low temperature regime: $T<T_{C1},T_{C2}$

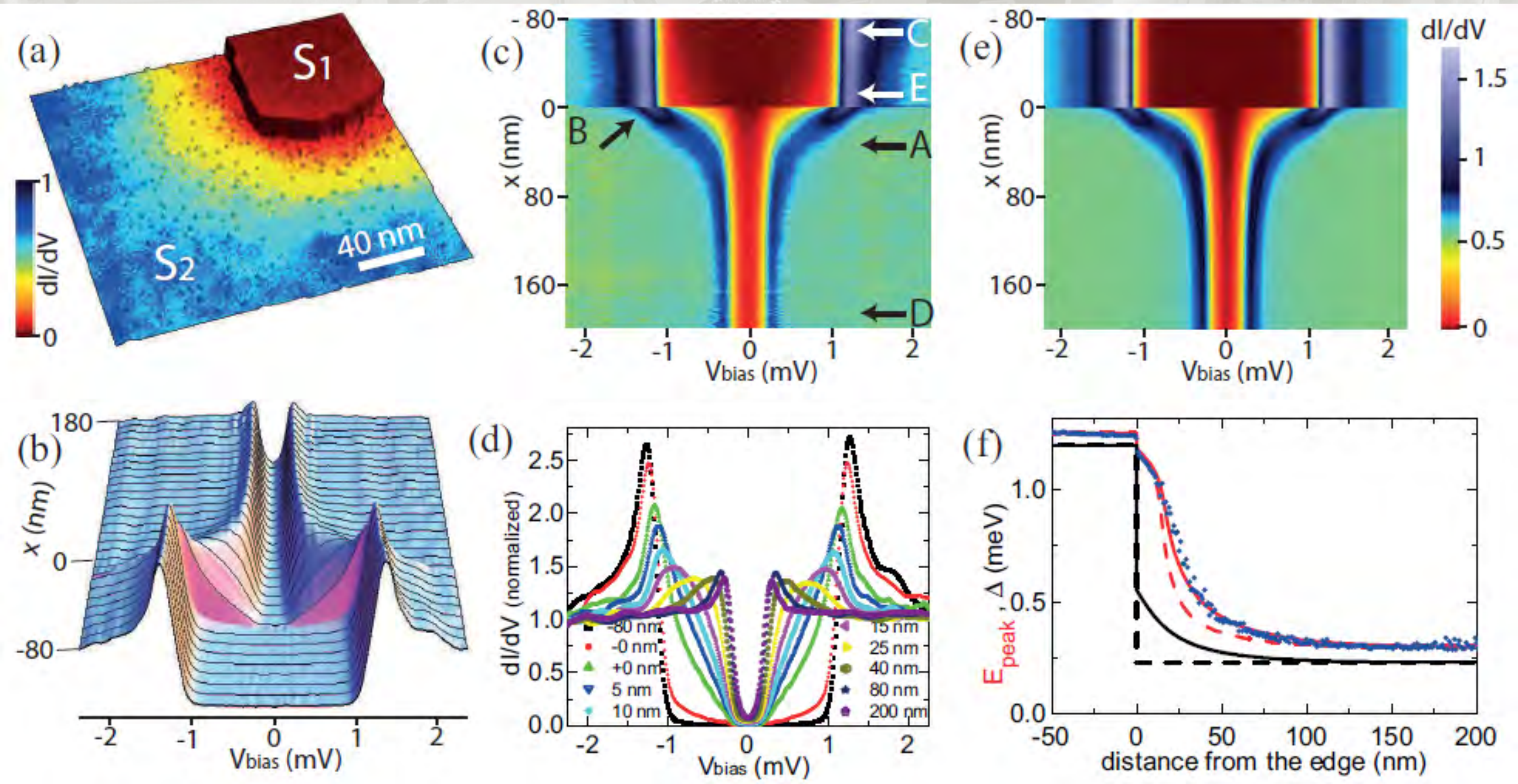

(Phys. Rev. X, 2014)

Josephson vortex matter in lateral proximity junctions

2.2. S-S': High temperature regime: $T_{C2}<T<T_{C1}$

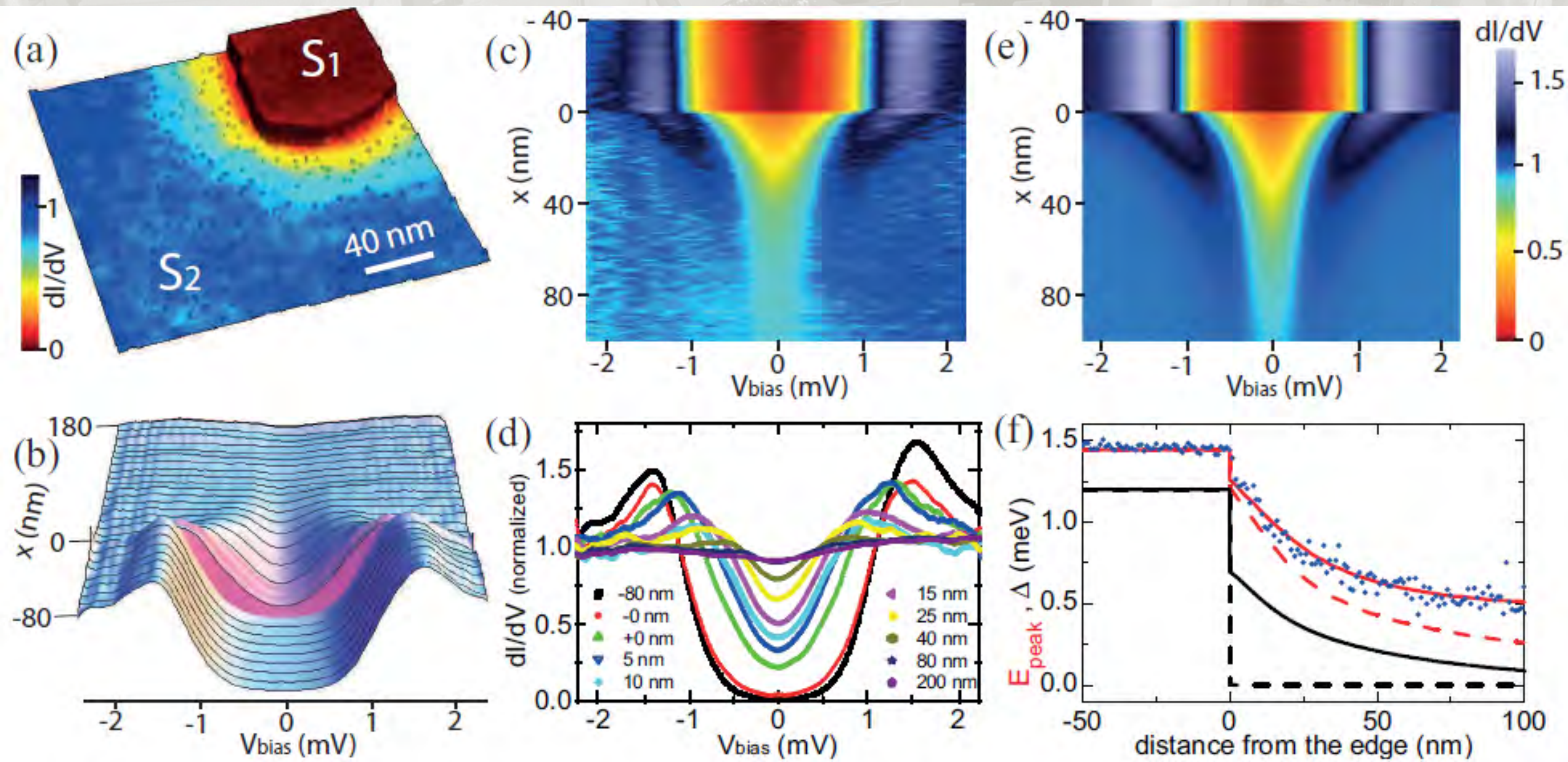

deGennes' prediction (1968) – experimentally demonstrated 2013

(Phys. Rev. X, 2014)

Josephson vortex matter in lateral proximity junctions

2.3. S-N: Lateral proximity effect in a disordered metal

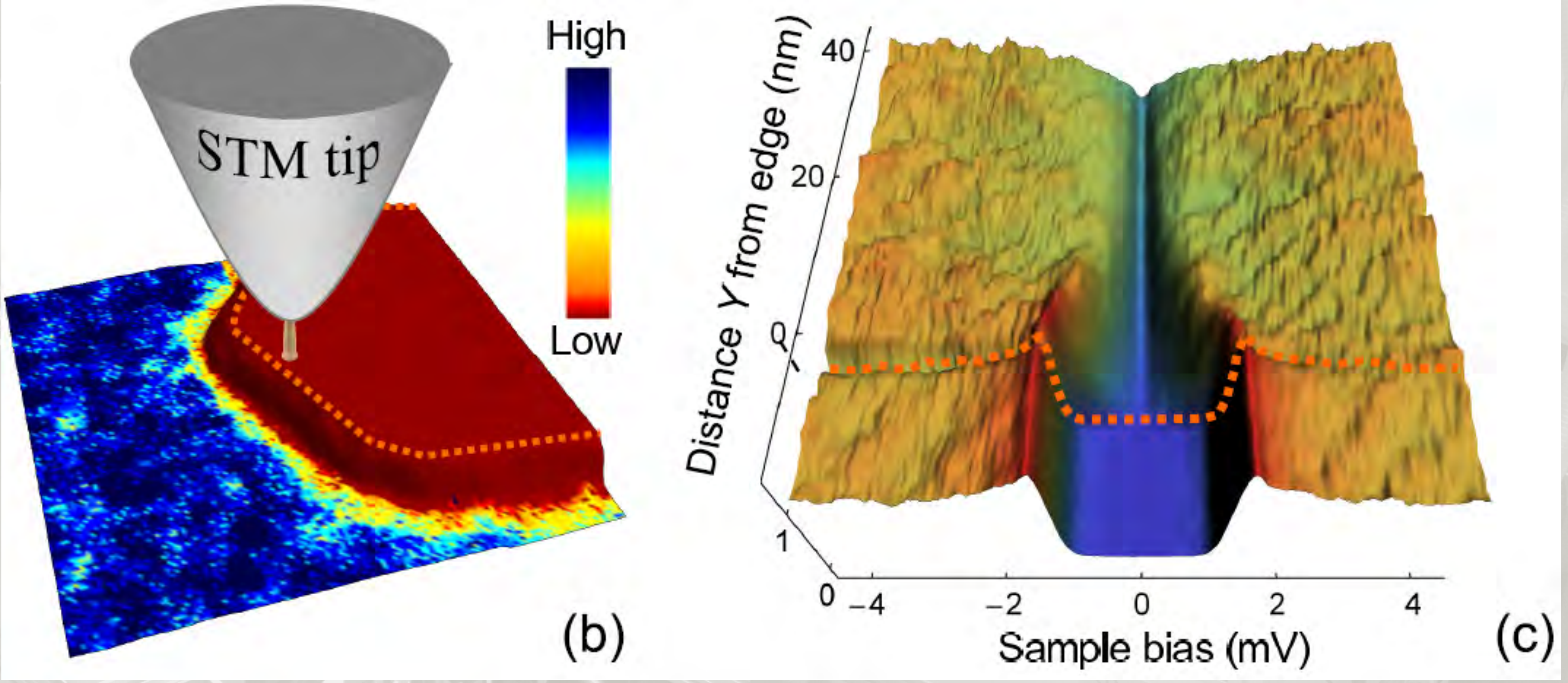

Josephson vortex matter in lateral proximity junctions

2.3. S-N: Lateral proximity effect in a disordered metal

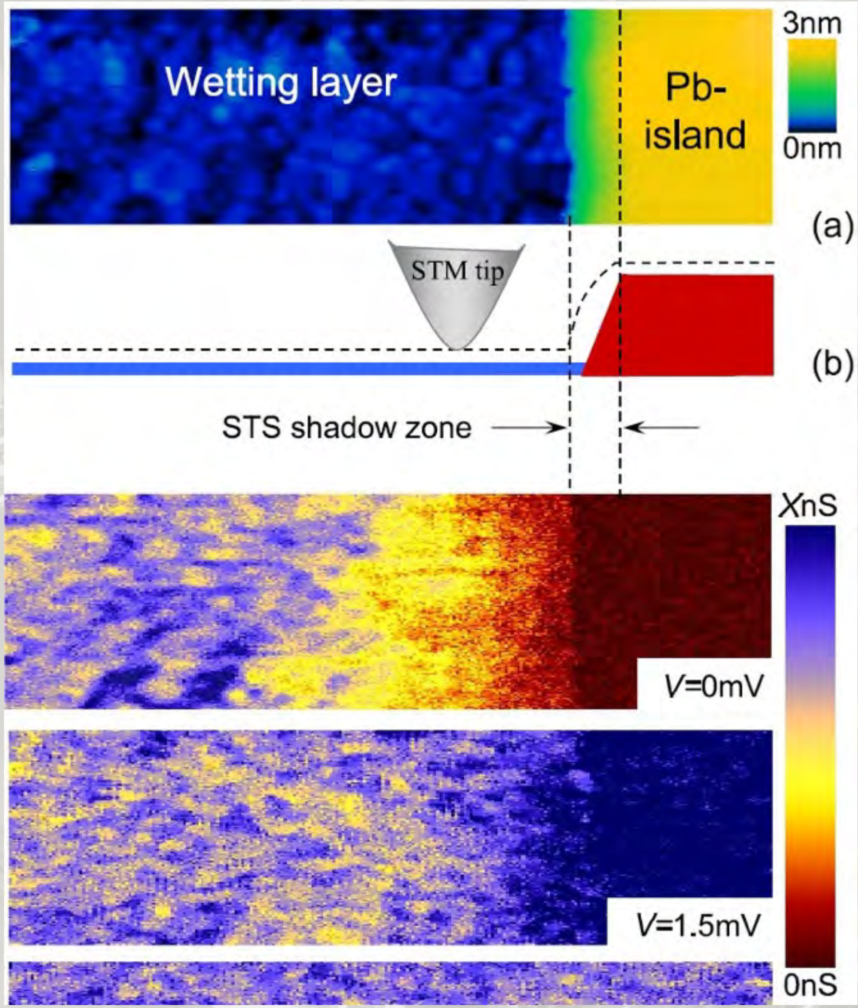

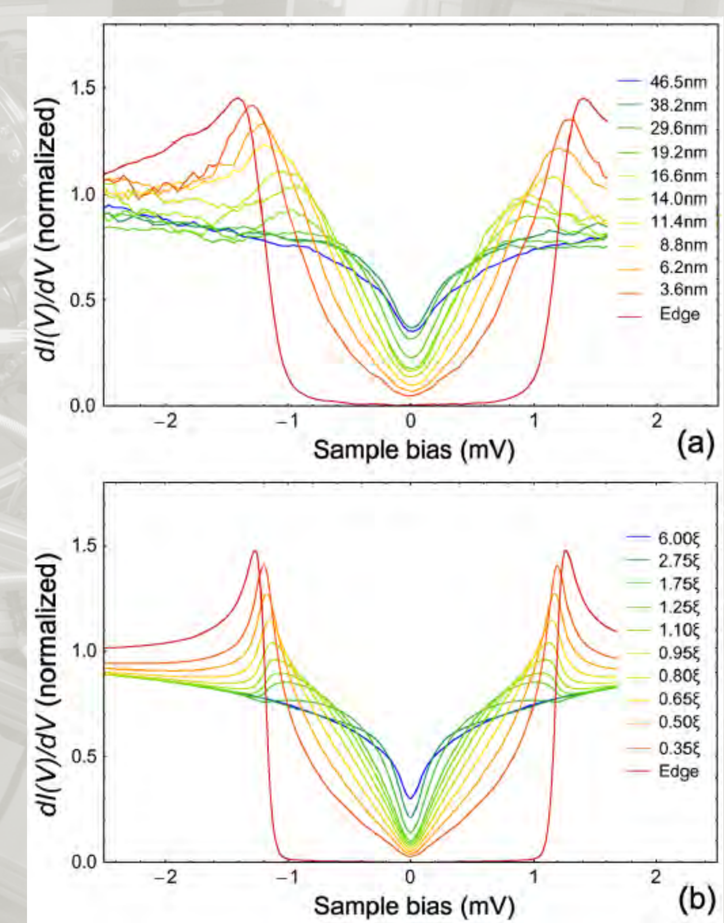

$\xi = (\hbar D / \Delta_{Pb})^{1/2} \approx 15nm$

L. Serrier-Garcia et al.
PRL (2013); PRX (2014)
Coll. J.-C. Cuevas, Madrid

Josephson vortex matter in lateral proximity junctions

2.3. S-N: Lateral proximity effect in a disordered metal

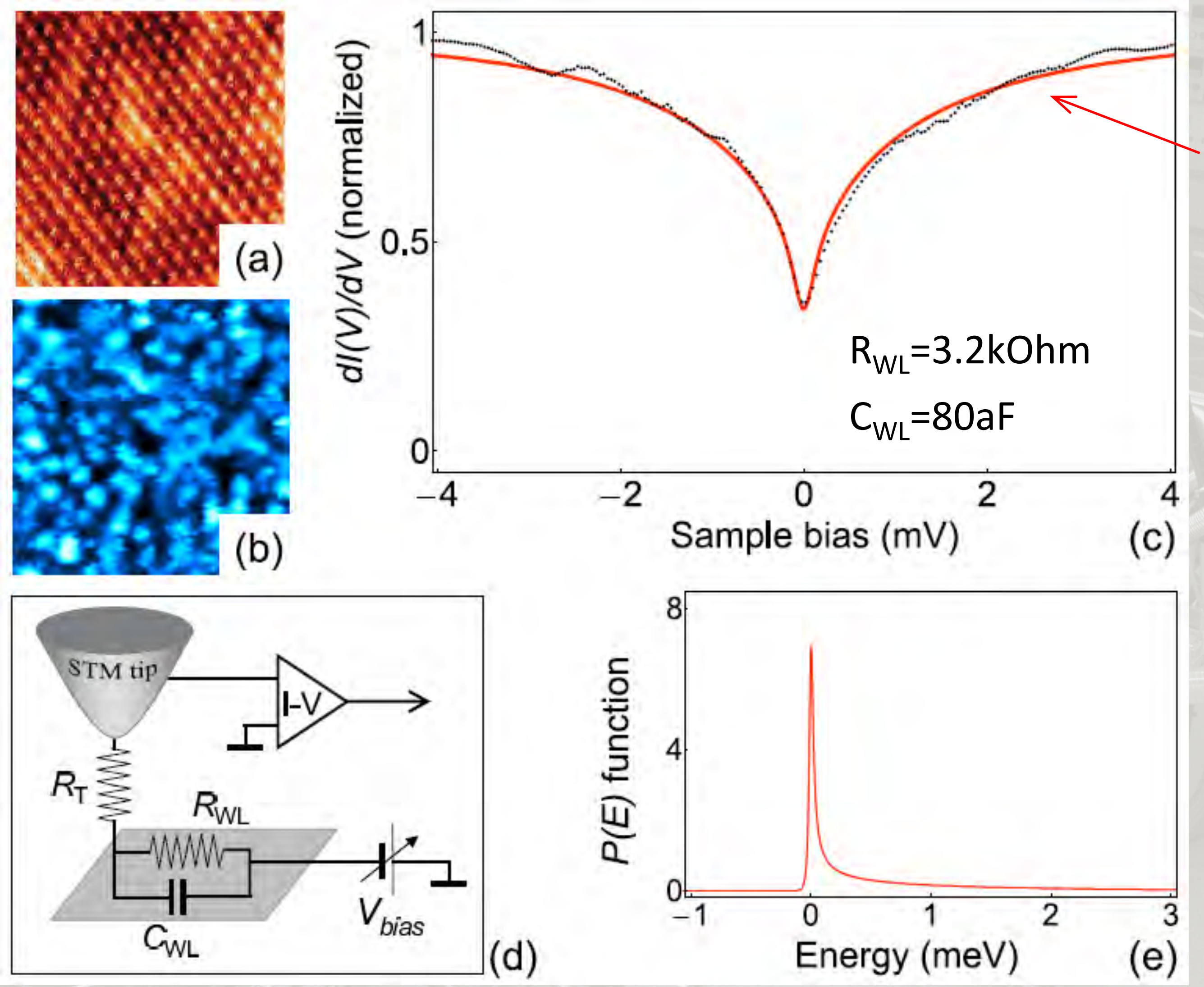

Josephson vortex matter in lateral proximity junctions

2.4. Lateral SNS Josephson junctions

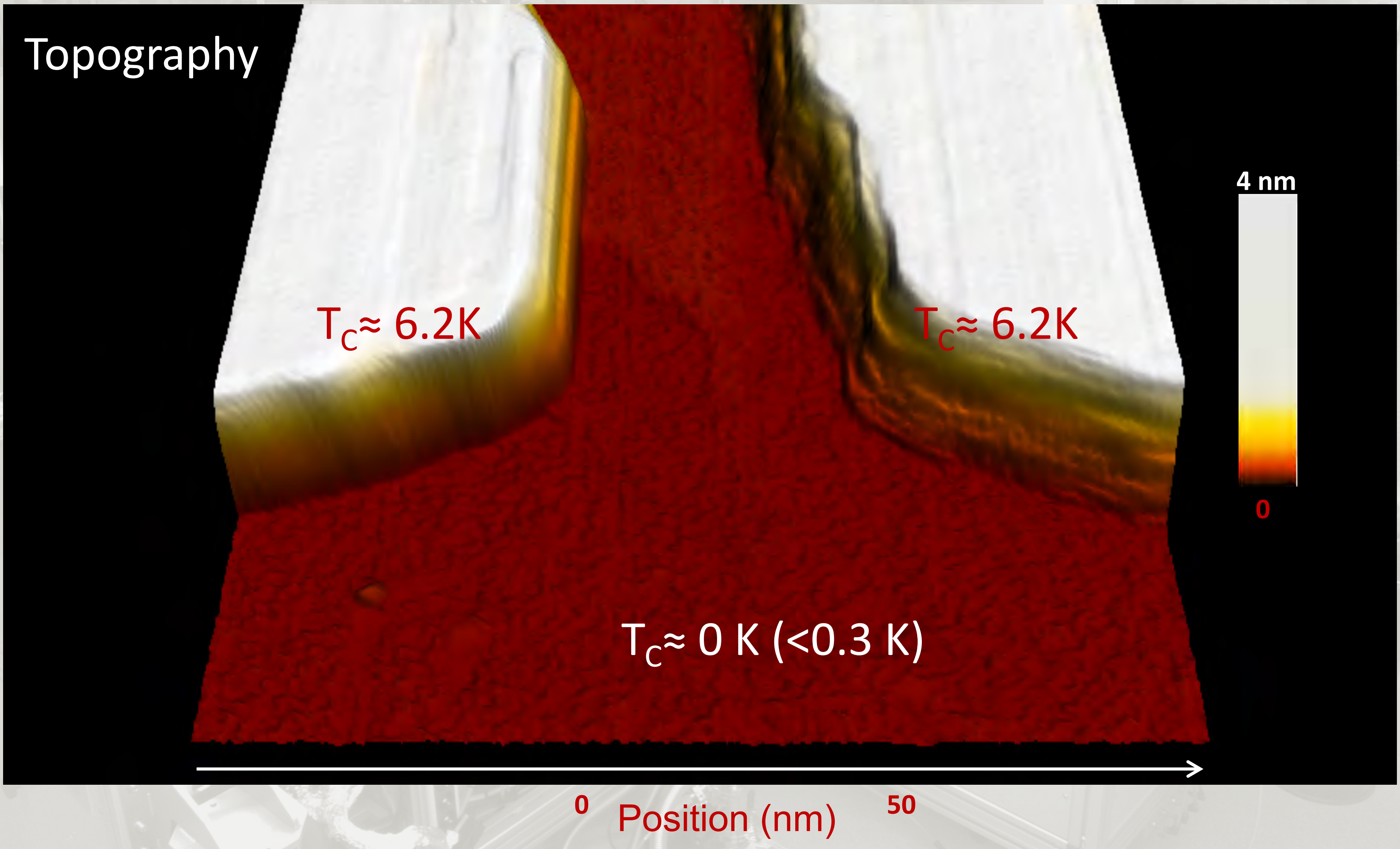

2/4

Josephson vortex matter in lateral proximity junctions

2.4. Lateral SNS Josephson junctions

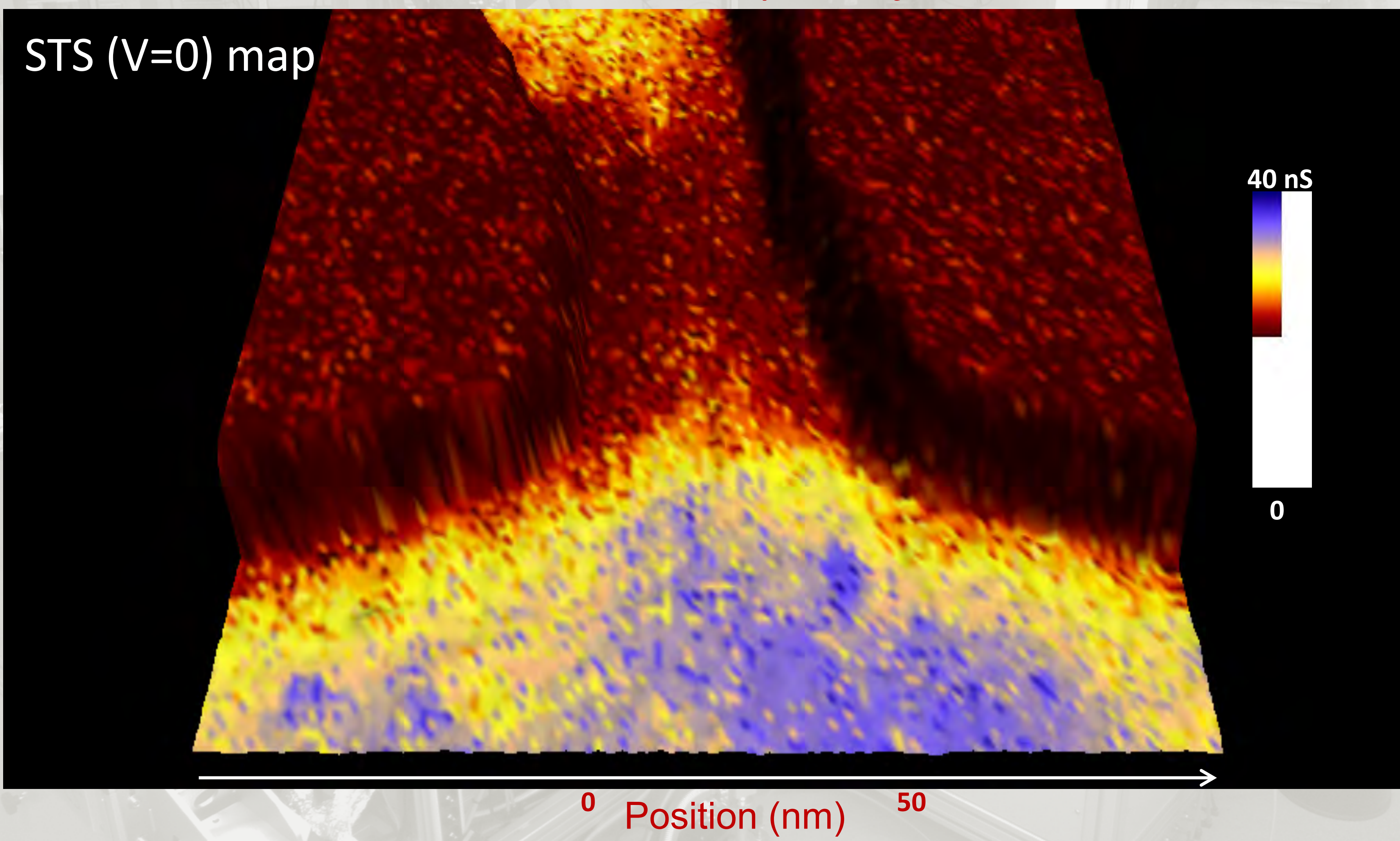

Proximity link is revealed between two close Pb-islands

Josephson vortex matter in lateral proximity junctions

2.4. Lateral SNS Josephson junctions

Line mode *dI/dV* spectroscopy

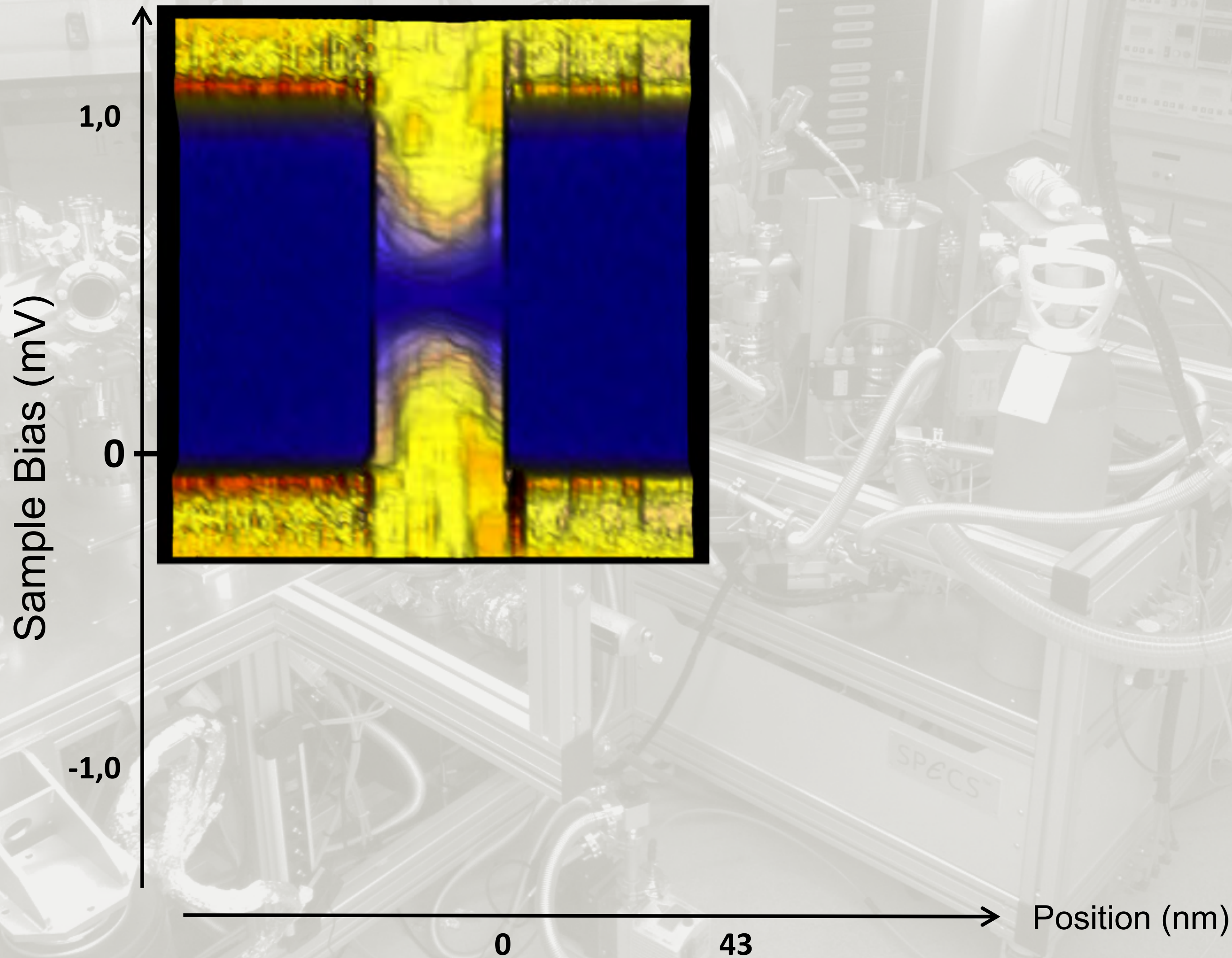

The mini-gap exists in the proximity region

Josephson vortex matter in lateral proximity junctions

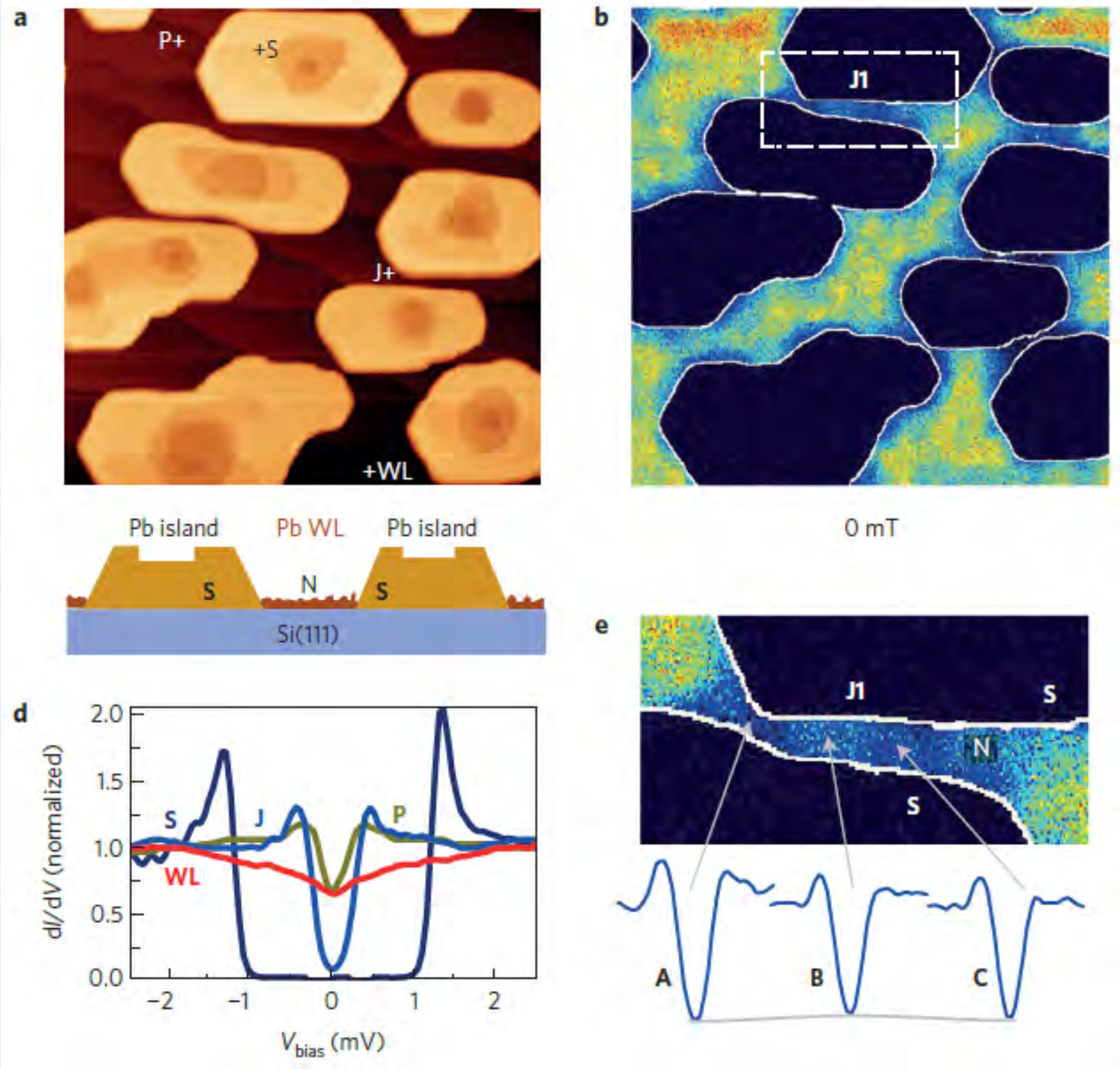

D. Roditchev et al.
Nat. Phys. 11, 332 (2015)

Josephson vortex matter in lateral proximity junctions

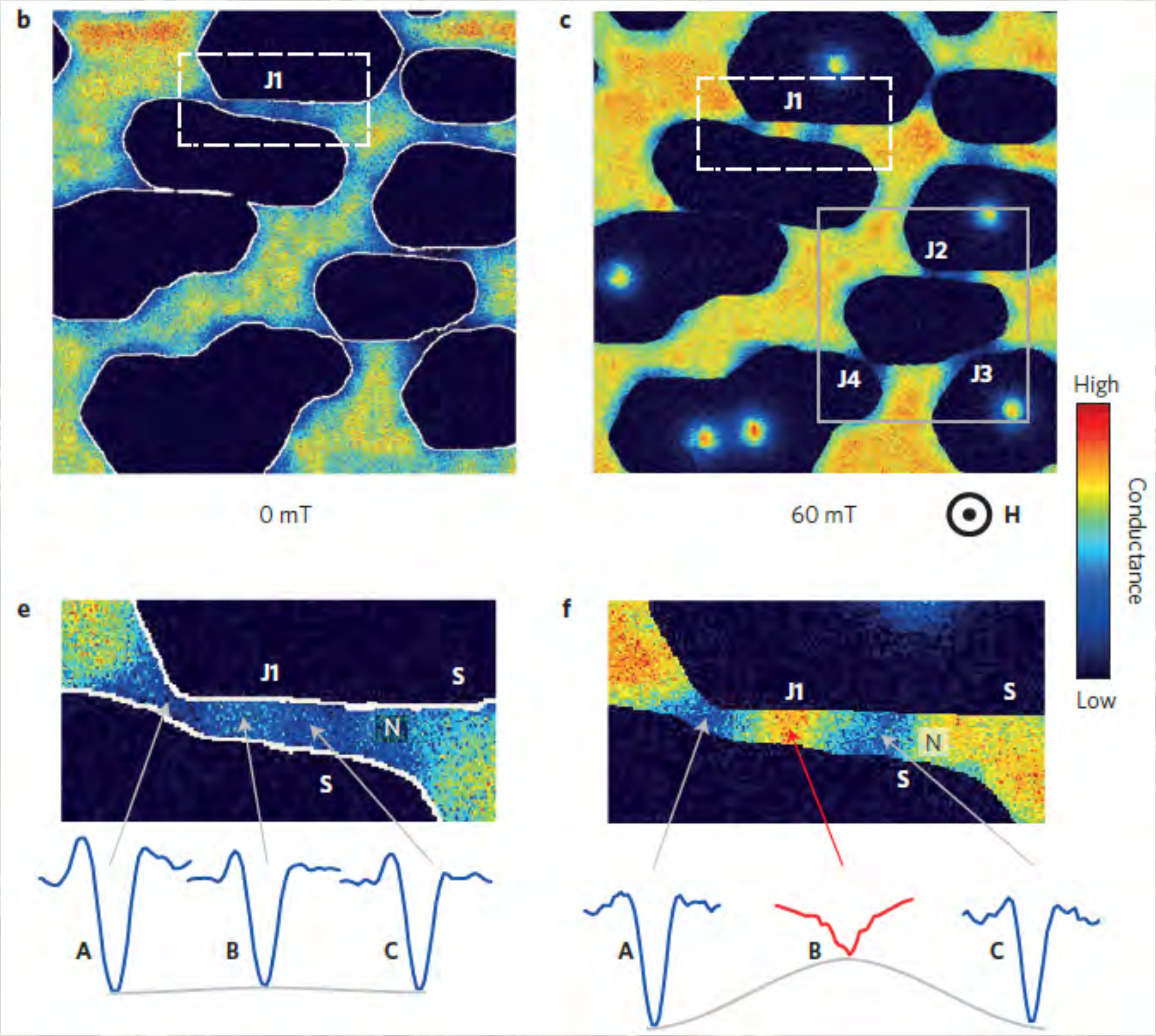

D. Roditchev et al. Nat. Phys. 11, 332 (2015)

Josephson vortex matter in lateral proximity junctions

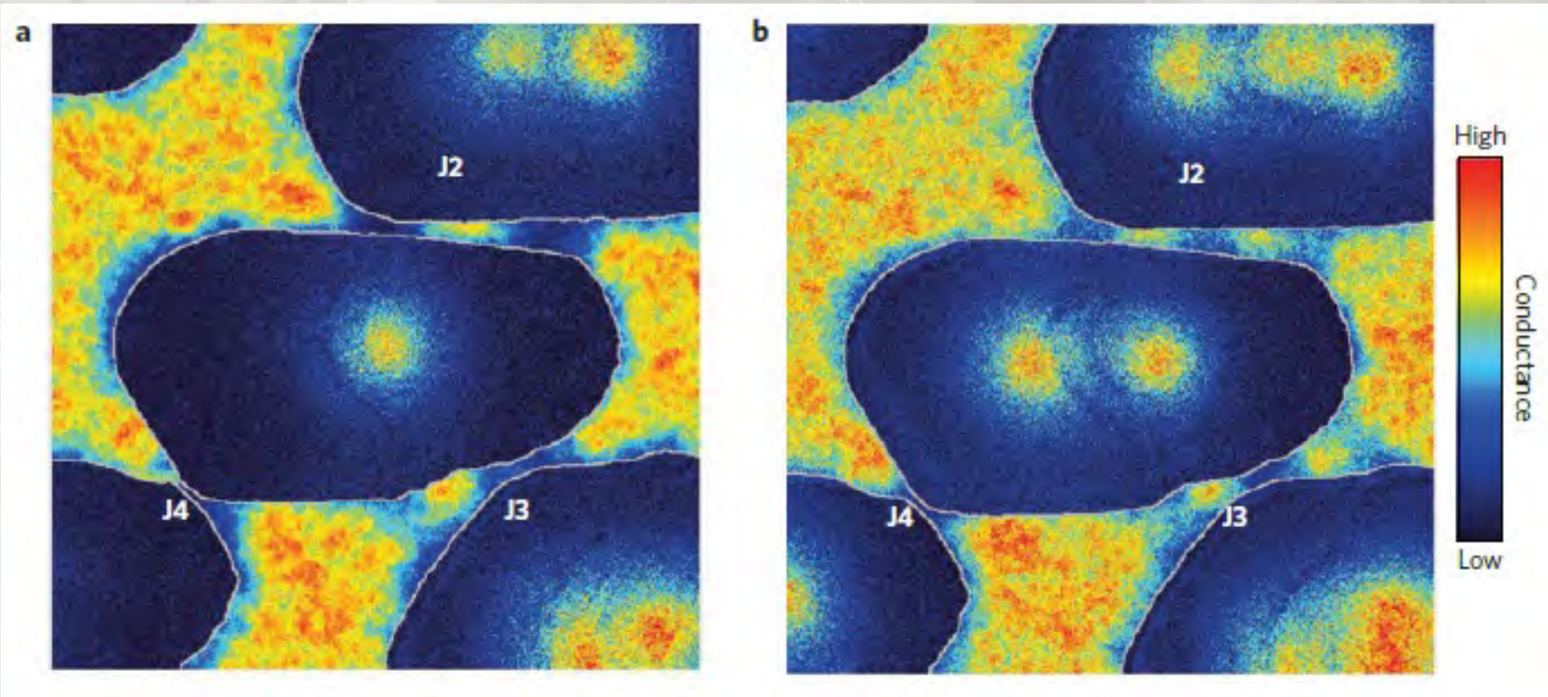

120mT 180mT

D. Roditchev et al.
Nat. Phys. 11, 332 (2015)

Josephson vortex matter in lateral proximity junctions

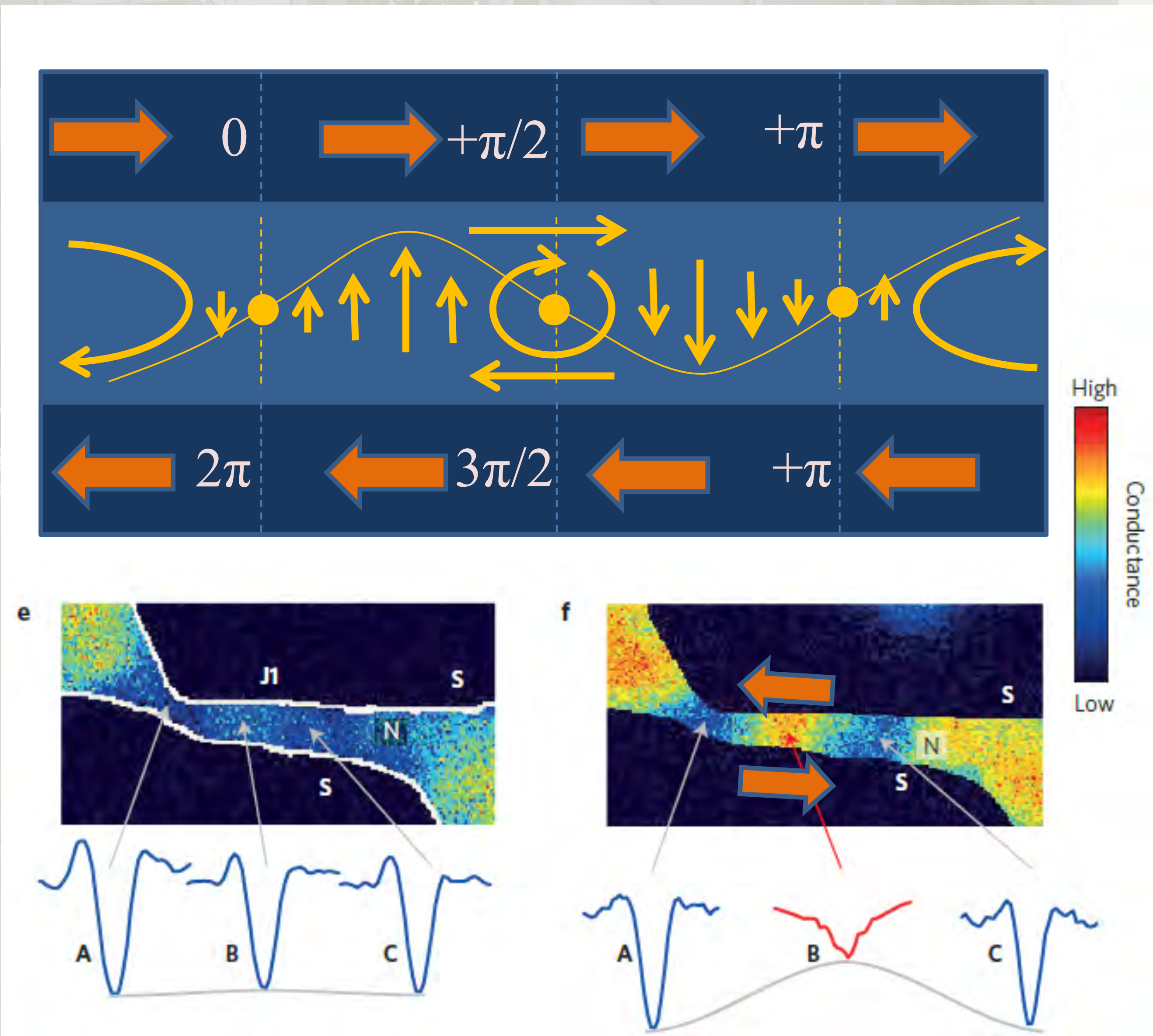

$j_{LOC}=j_C \sin(\Delta\varphi)$

D. Roditchev et al. Nat. Phys. 11, 332 (2015)

Josephson vortex matter in lateral proximity junctions

2.5. Modelling: GL theory + correlation function

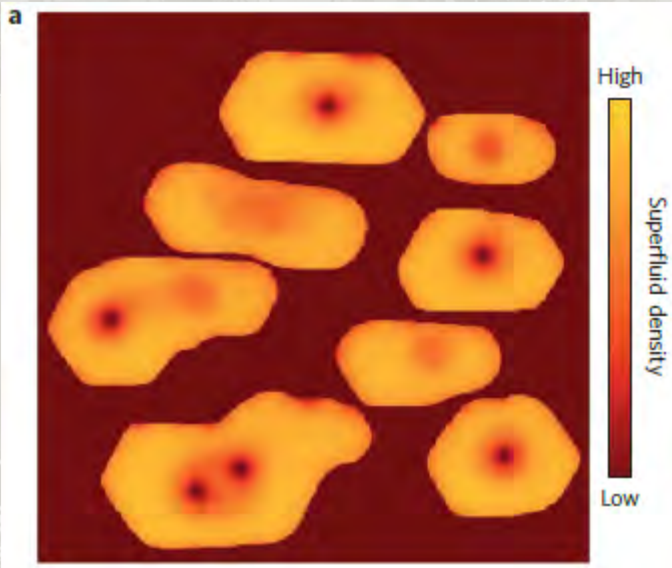

GL theory

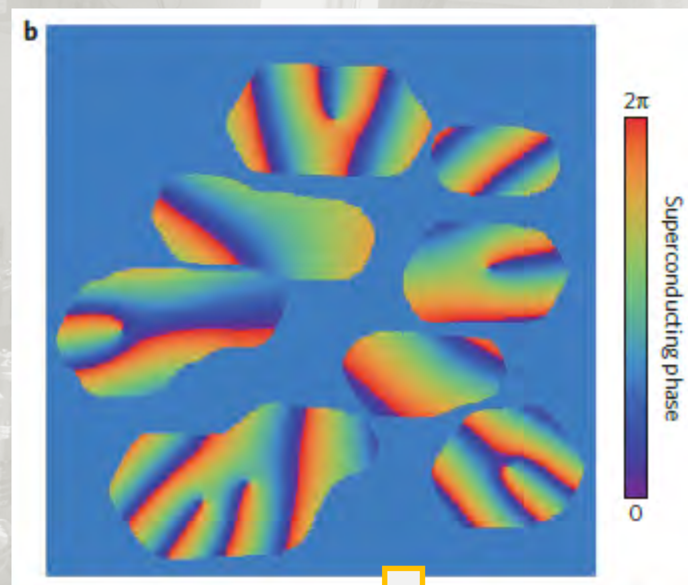

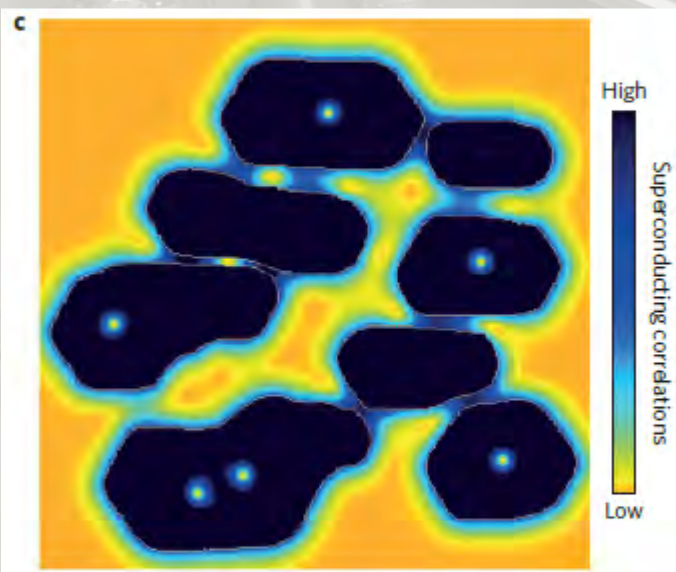

$$\phi(\vec{r}) \propto \sum_i \int_{C_i} e^{-\frac{|\vec{r}-\vec{r}_i|}{2\xi}} e^{i\,\varphi^*(\vec{r},\vec{r}_i)} dl,$$

with gauge-invariant phase difference:

$$\varphi^*(\vec{r},\vec{r}_i) = \varphi(\vec{r}_i) + \frac{2\,\pi}{\phi_0} \int_{\vec{r}_i}^{\vec{r}} \overrightarrow{A}.\overrightarrow{dl}$$

M. Milosevic & T. Cren in Nat. Phys. (2015)

Gauge-Independent Phase Difference

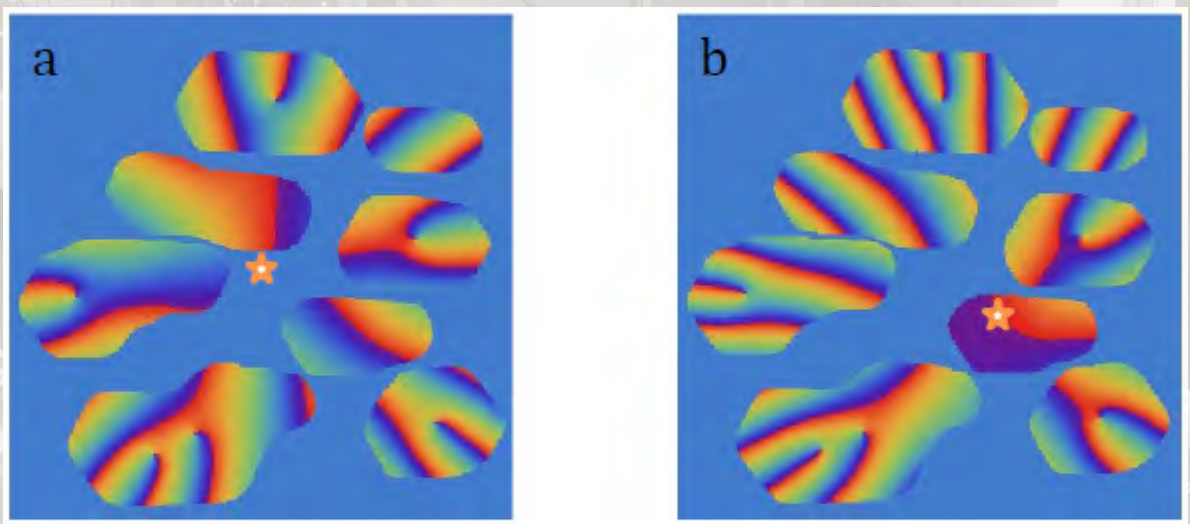

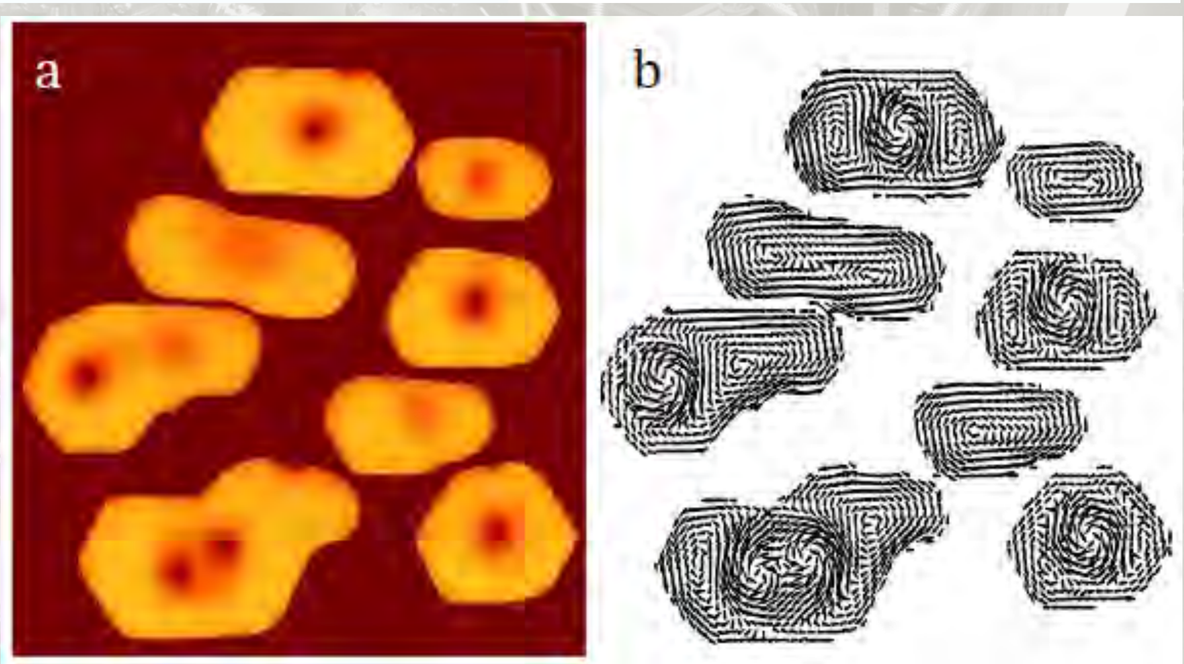

Self-Consistent location of Josephson vortices

Since the islands are independent, their gauge-independent phase portraits also are. There is an arbitrary global phase difference between each pair of islands. It decides where JV are located inside junctions.

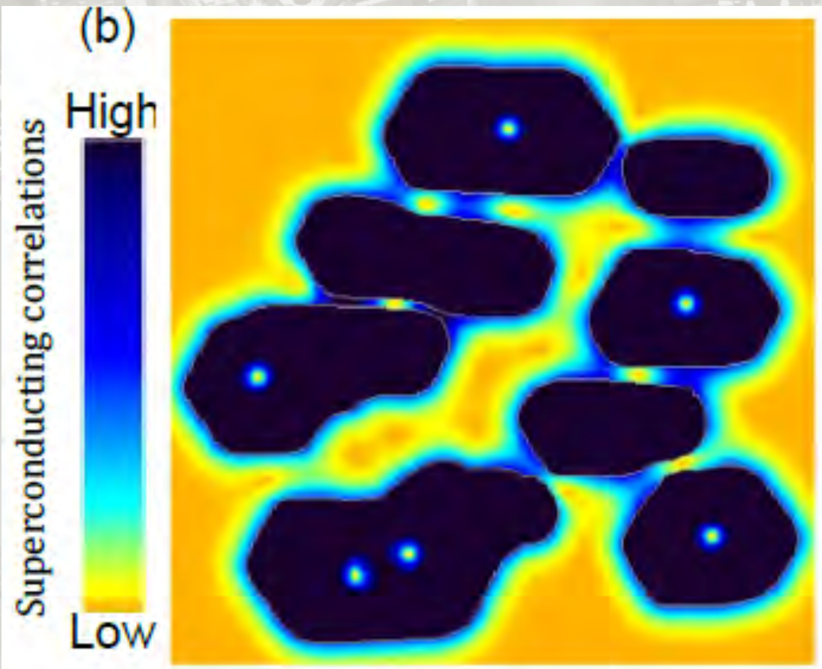

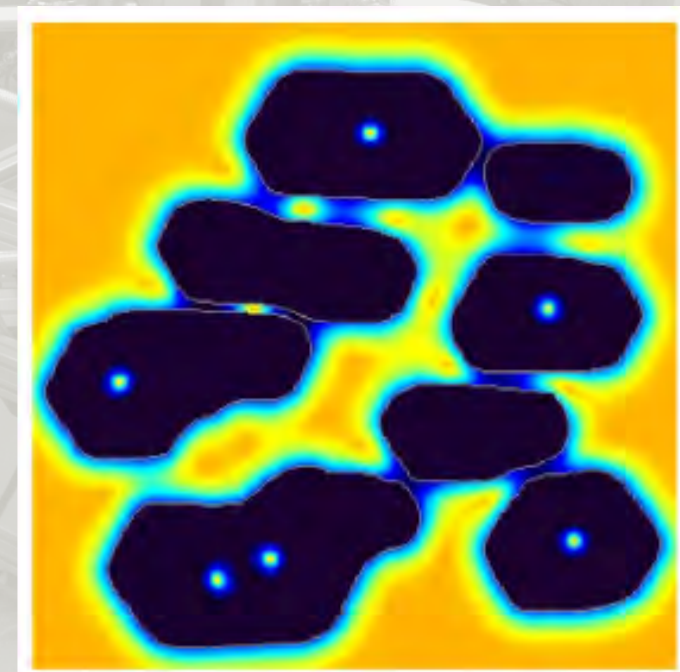

Self-Consistent location of Josephson vortices

For each pair of islands the total current crossing each junction and corresponding kinetic energy are calculated as a function of global phase difference $\Delta\phi_0$. The exact position of JV is obtained when ***j_{TOT}****=0* and ***E_C****=Min{Ec($\Delta\phi_0$)}*.

$$\vec{j}(\vec{r}) = \frac{2e}{2m}|\phi(\vec{r})|^2(\hbar\vec{\nabla}\theta + 2e\vec{A}),$$

$$E_c = \iint_{N\,region} \frac{1}{2m}\left|(-i\hbar\vec{\nabla} + 2e\vec{A})\phi(\vec{r})\right|^2 d\vec{r}.$$

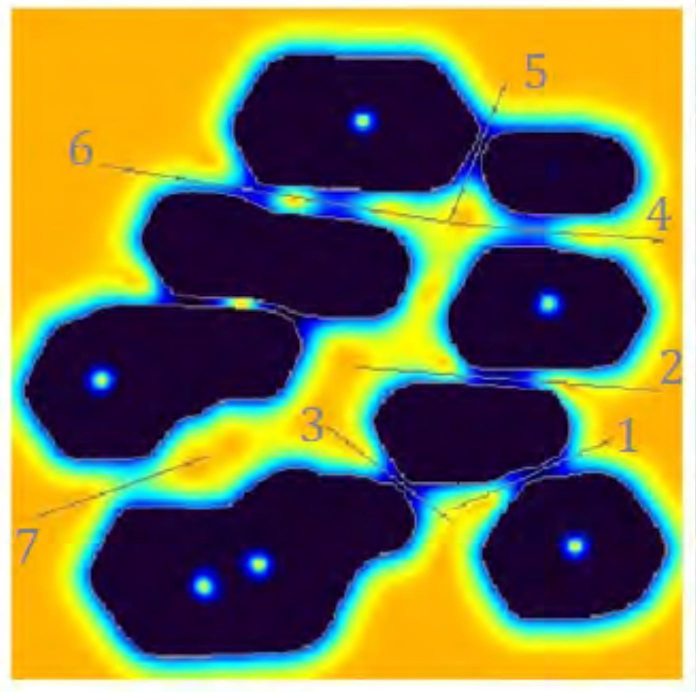

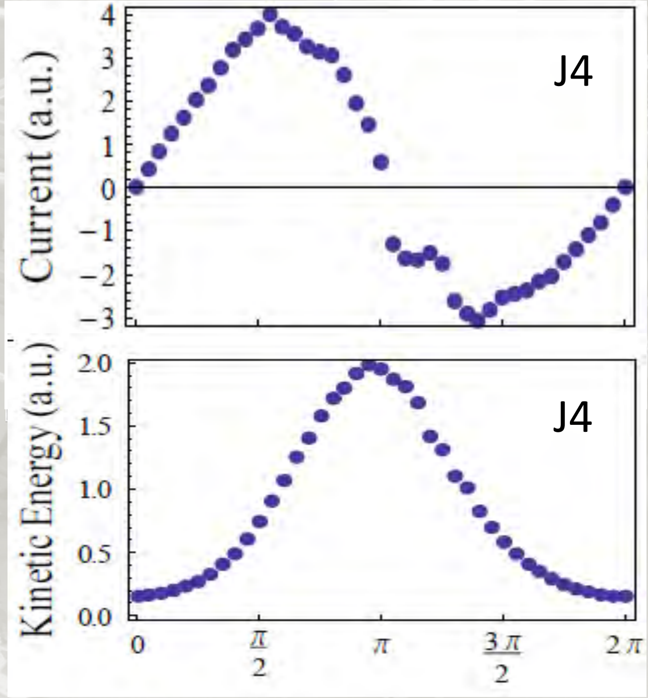

Josephson vortex matter in lateral proximity junctions

Modelling vs Experiment: Result

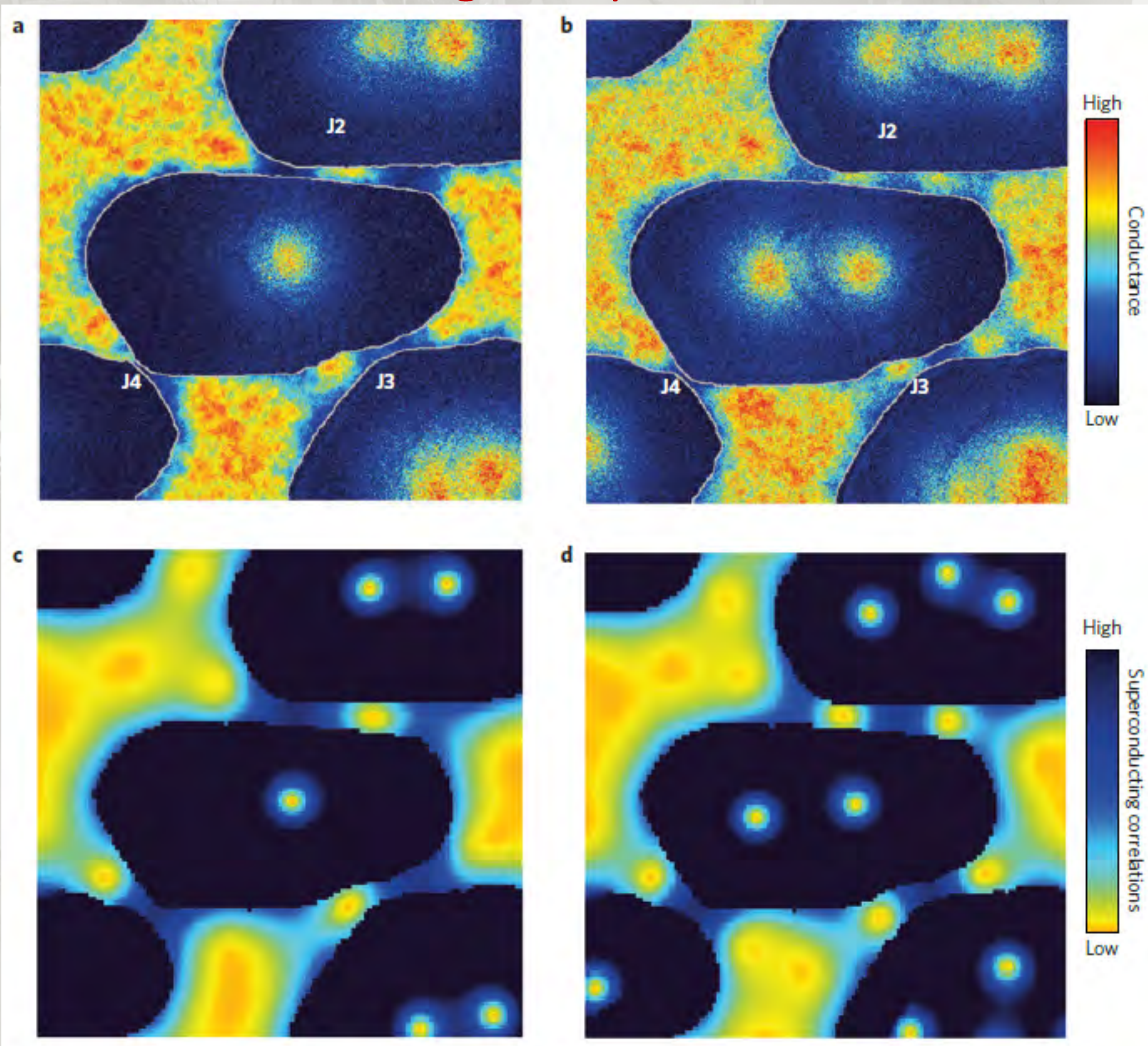

D. Roditchev et al. Nat. Phys. 11, 332 (2015)

Josephson vortex matter in lateral proximity junctions

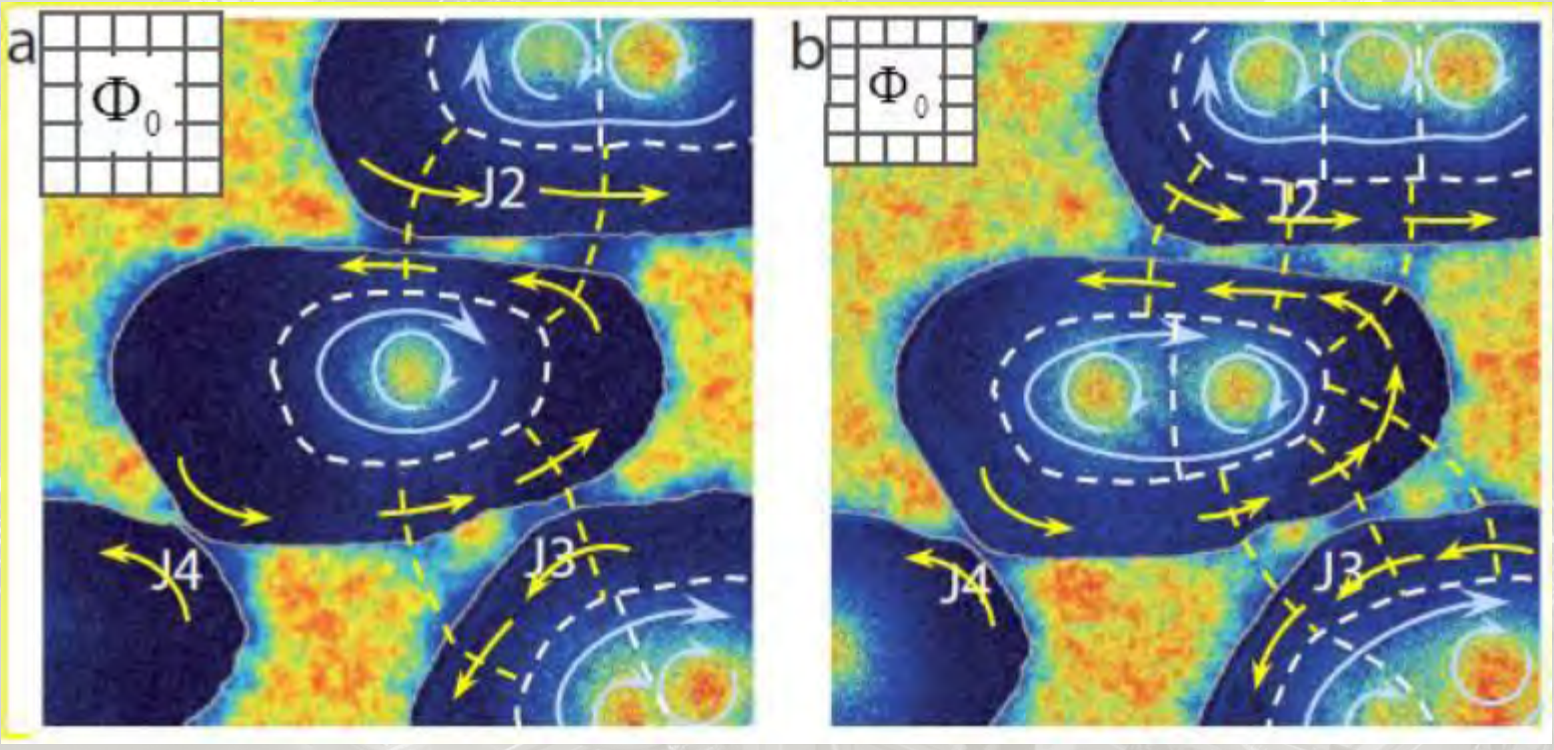

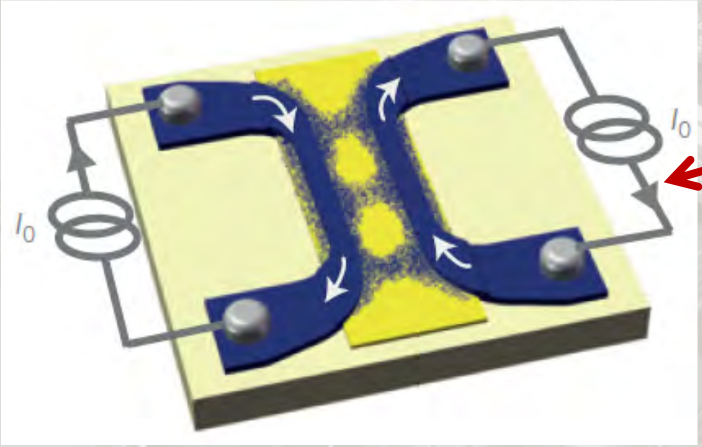

Suggested SNS nano-device

D. Roditchev et al.
Nat. Phys. 11, 332 (2015)

Conclusions 2/4

Cores of Josephson vortices are revealed in lateral SNS proximity junctions. The Josephson vortices have purely interference origin.

Similarly to vortices in thin superconductors (Pearl vortex), Josephson vortices do not require magnetic screening to exist – novel phase-controlled devices

Josephson vortices in SIS junctions may also have cores !

Outlook

Elementary excitations and vortex in superconducting **Pb-monolayers** *Nat. Phys. (2014)*

Josephson vortex matter in **proximity** junctions *PRL (2013), PRX (2014), Nat. Phys. (2015)*

Long-range Shiba bound states in 2D limit *Nat. Phys. (2015)*

Unconventional **collective** bound states *(2017) to be published*

Institut des NanoSciences de Paris

Long-range Shiba bound states

Yu-Shiba-Rusinov (YSR) problem:
3D scattering on a classical spin $\vec{S}$

L. Yu. Acta Phys. Sin (1965)

H. Shiba. Prog. Th. Phys. (1968)

A. I. Rusinov JETP Lett. (1969)

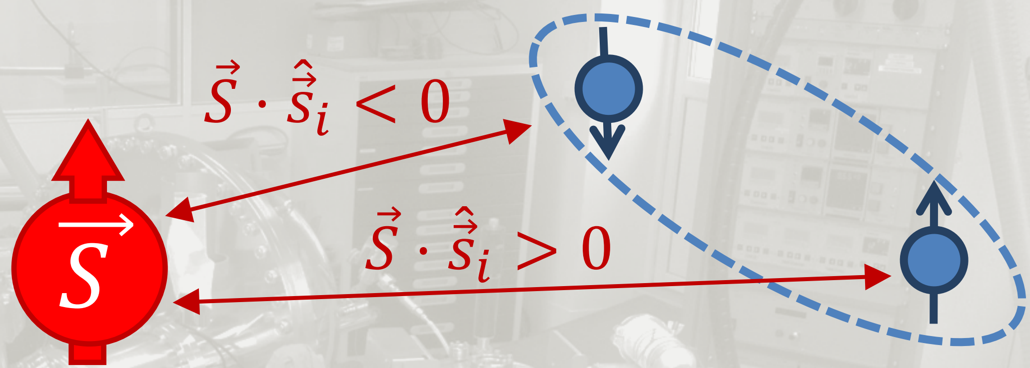

Two terms hamiltonian: magnetic and non-magnetic scattering

$$H_{Imp} = -\frac{JS}{2}(c^\dagger_{0\uparrow}c_{0\uparrow} - c^\dagger_{0\downarrow}c_{0\downarrow}) + K(c^\dagger_{0\uparrow}c_{0\uparrow} + c^\dagger_{0\downarrow}c_{0\downarrow})$$

$$E_{Shiba} = \pm\Delta\cos\left(\delta^+ - \delta^-\right)$$ where $\tan\delta^\pm = K\nu_0 \pm \frac{JS}{2}\nu_0$

$$\psi_\pm(r) = \frac{1}{\sqrt{N}}\frac{\sin\left(k_F r + \delta^\pm\right)}{k_F r}e^{-\Delta\sin(\delta^+ - \delta^-)r/\hbar v_F}$$

valid for $k_F\, r \gg 1$

$$\boxed{\frac{\Delta}{\hbar v_F} \approx \xi^{-1}}$$

Long-range Shiba bound states

Mn on Nb(110) (bulk)

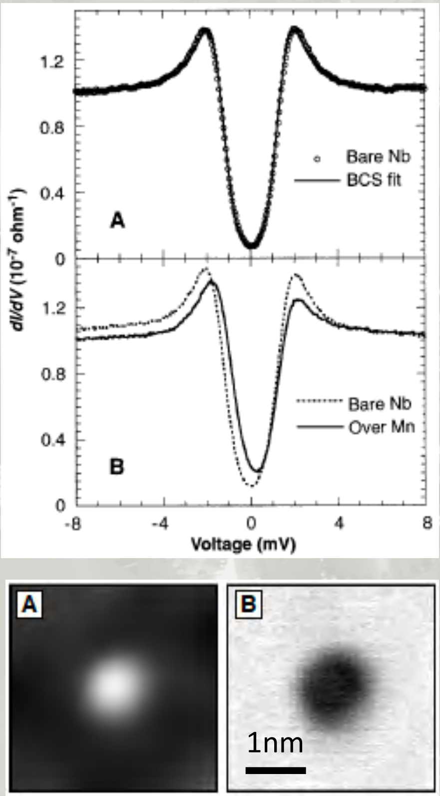

A. Yazdani et al. Science (1997)

Mn and Cr on Pb(111) (20ML)

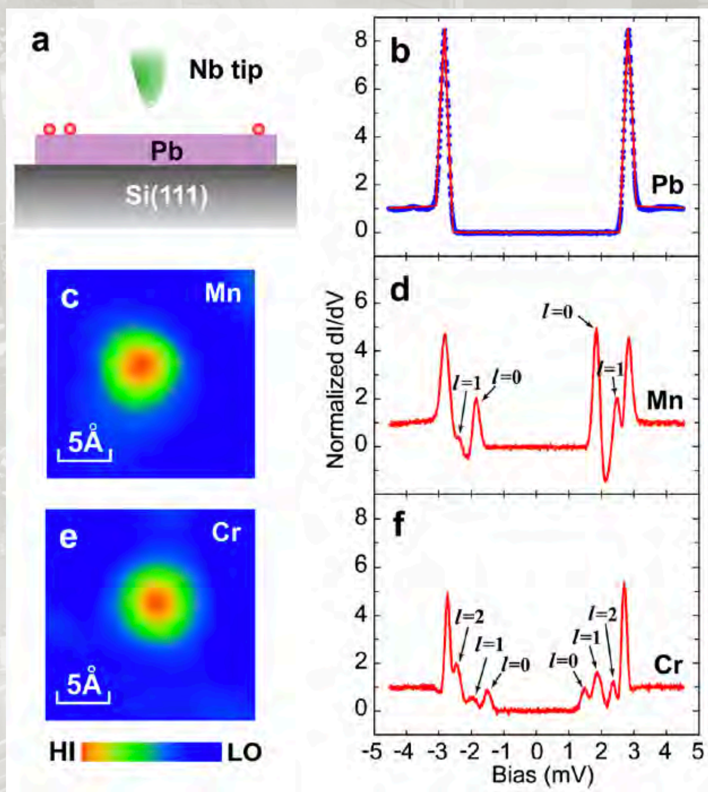

Shuai-Hua Ji, PRL (2008)

Cr on Pb(111) (300nm)

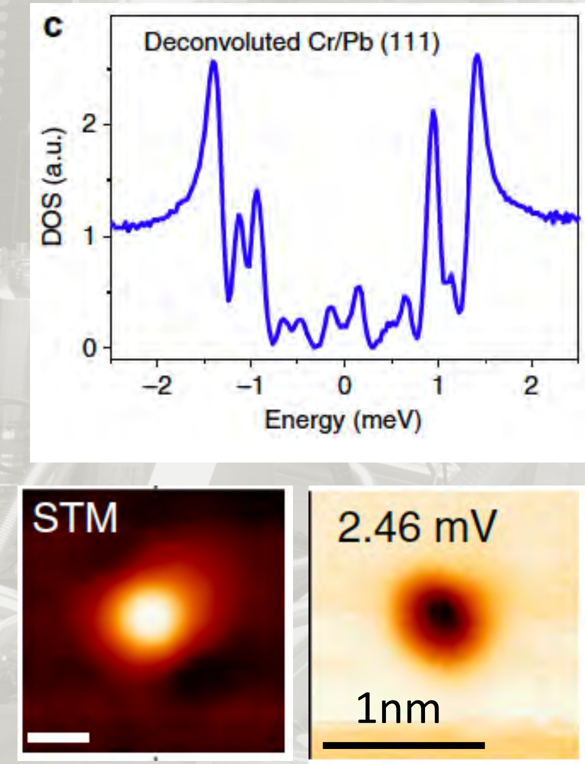

D.-J. Choi et al. Nat. Comm. (2017)

$$\psi_{\pm}(r) = \frac{1}{\sqrt{N}} \frac{\sin\left(k_F r + \delta^{\pm}\right)}{k_F r} e^{-\Delta \sin(\delta^{+}-\delta^{-}) r/\hbar v_F}$$

valid for $k_F\, r \gg 1$

Long-range Shiba bound states – *2H-NbSe$_2$*

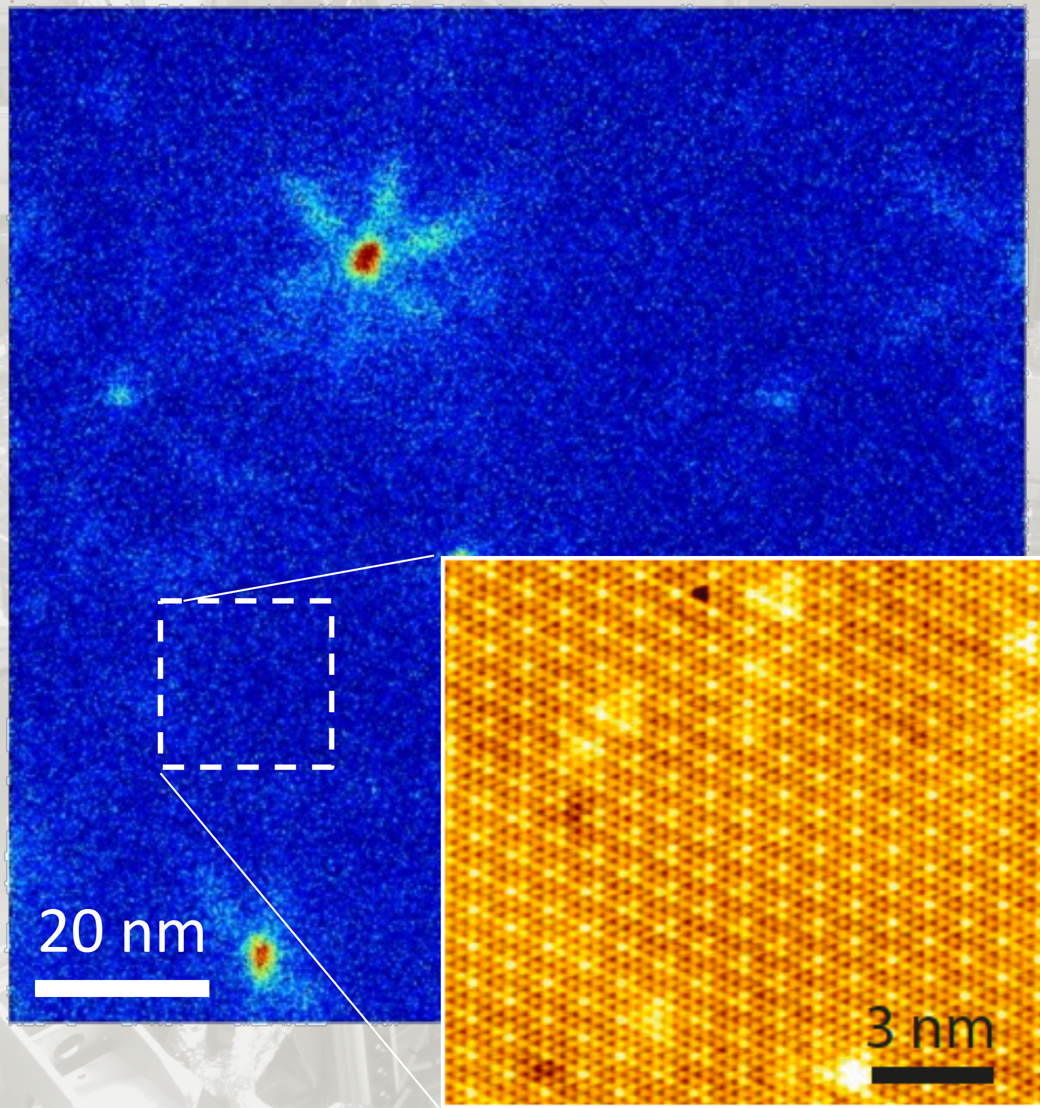

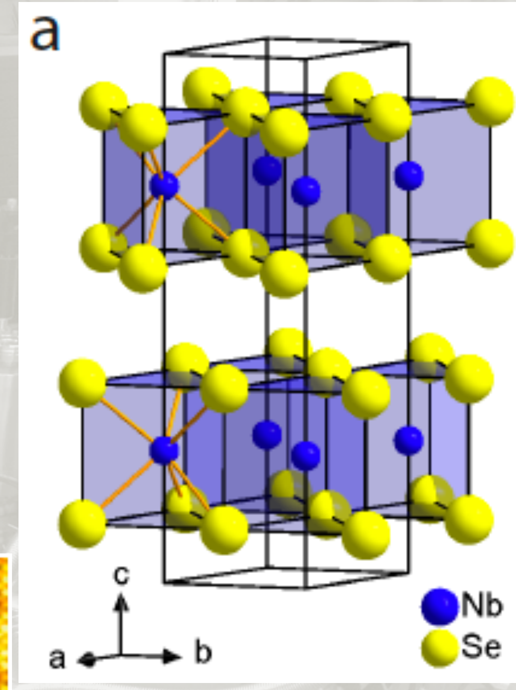

Magnetic impurities:
175 ppm of Fe,
54 ppm of Cr
22 ppm of Mn

G. Ménard et al, Nat. Phys. (2015)

Long-range Shiba bound states – *2H-NbSe$_2$*

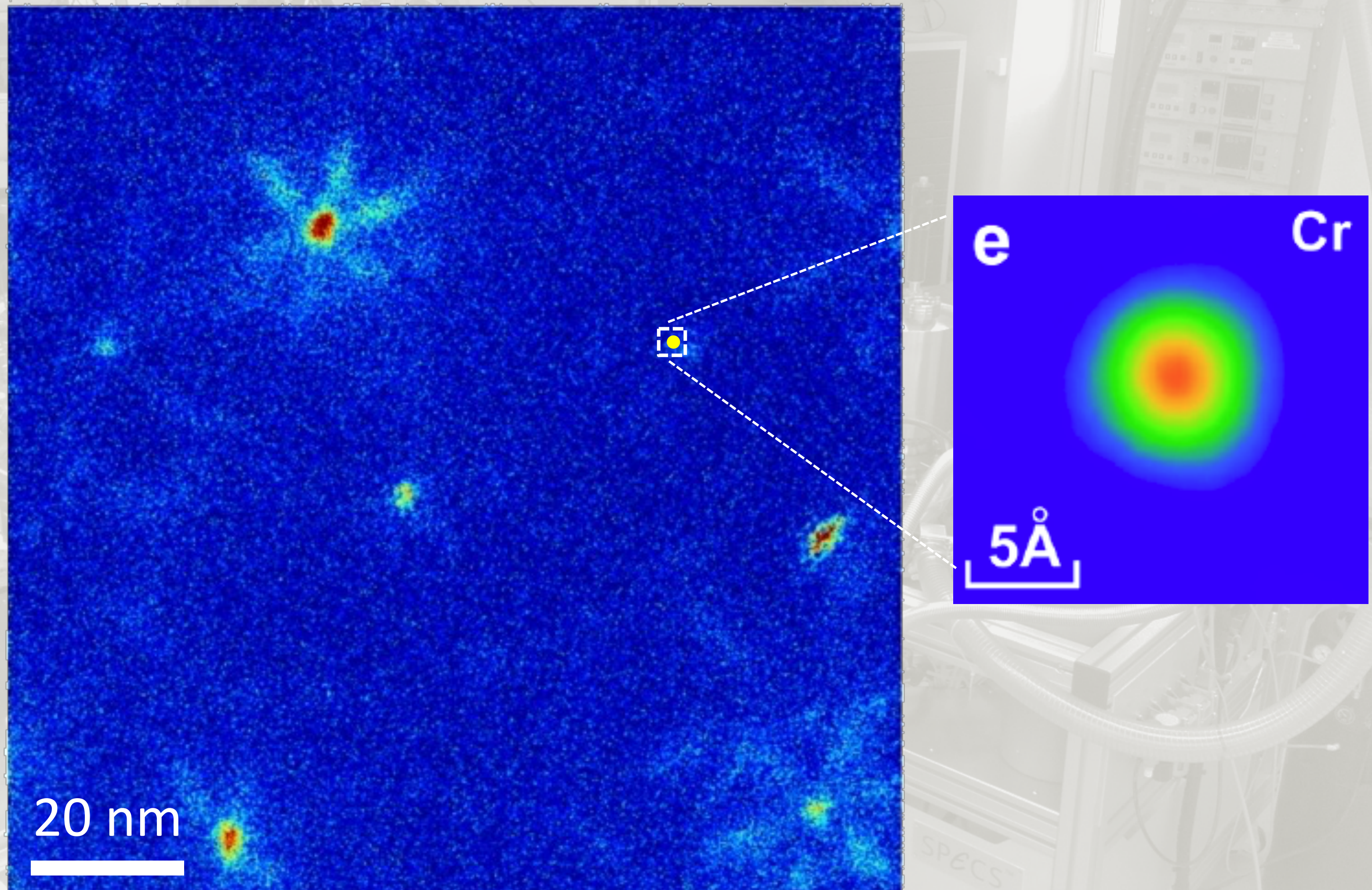

In-gap spectroscopy reveals large scale star shaped features

G. Menard et al, Nat. Phys. (2015)

Long-range Shiba bound states – *2H-NbSe$_2$*

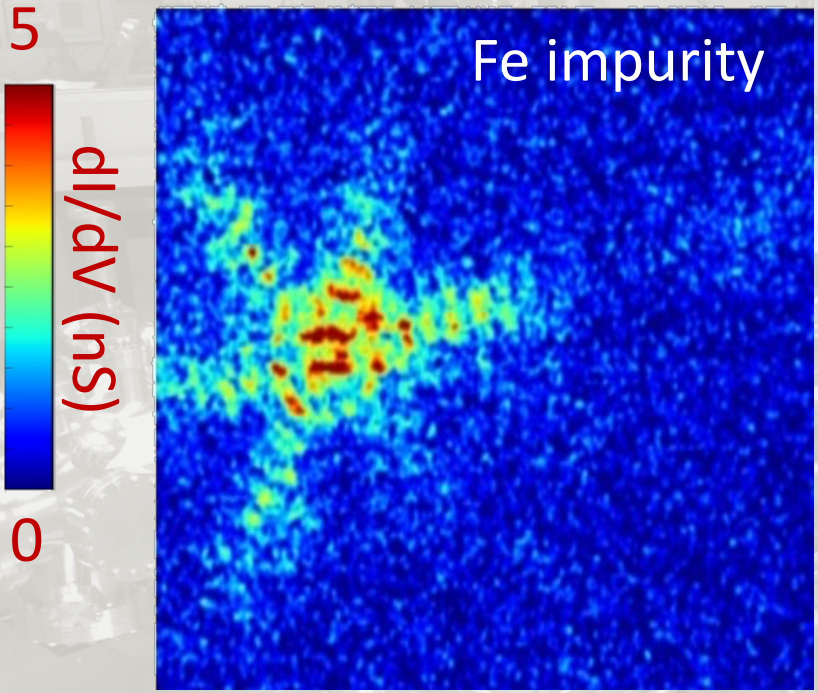

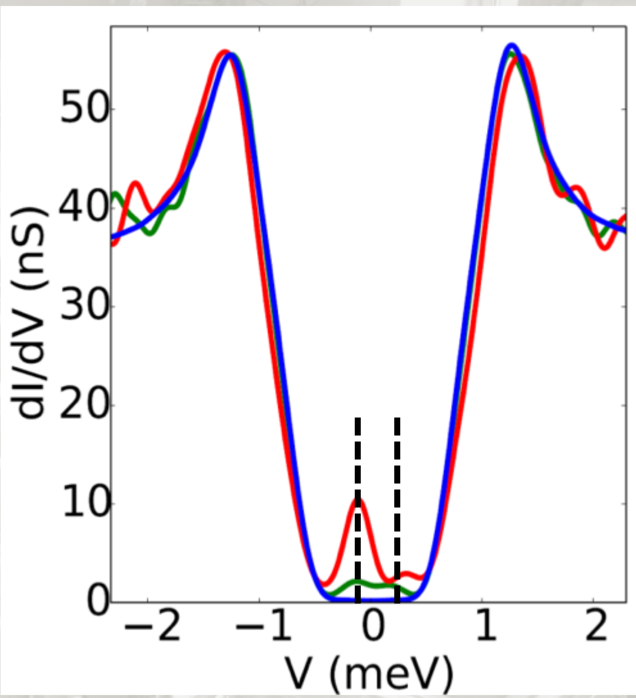

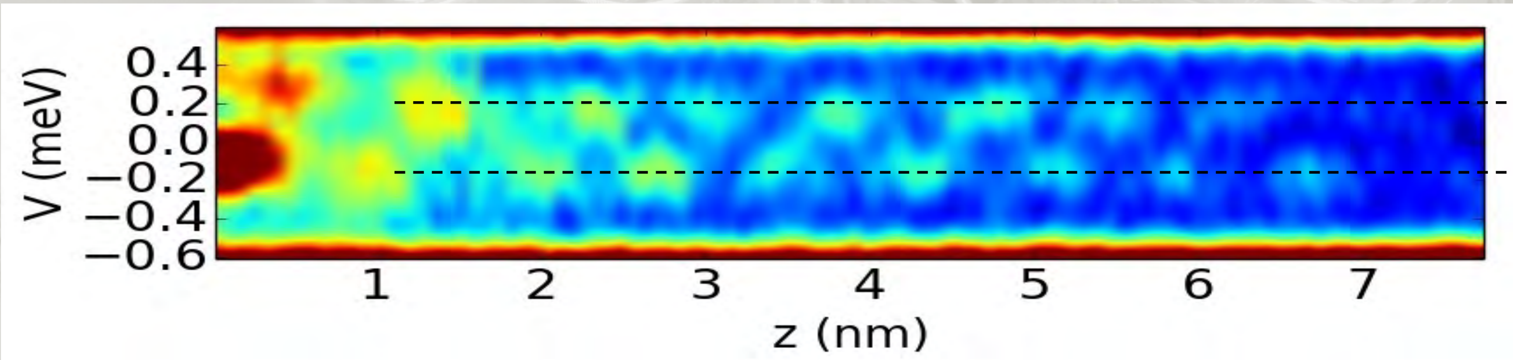

There are 2 Shiba peaks. They oscillate in space with a phase shift.

Long-range Shiba bound states – *2H-NbSe$_2$*

$$\psi_\pm = \frac{1}{\sqrt{N\pi k_F r}} \sin\left(k_F r - \frac{\pi}{4} + \delta^\pm\right) e^{-\sin(\delta^+ - \delta^-) r\Delta/\hbar v_F}$$

$$E_S = \Delta\cos(\delta^+ - \delta^-)\,; \quad \tan\delta^\pm = K\nu_0 \pm \frac{JS}{2}\nu_0$$

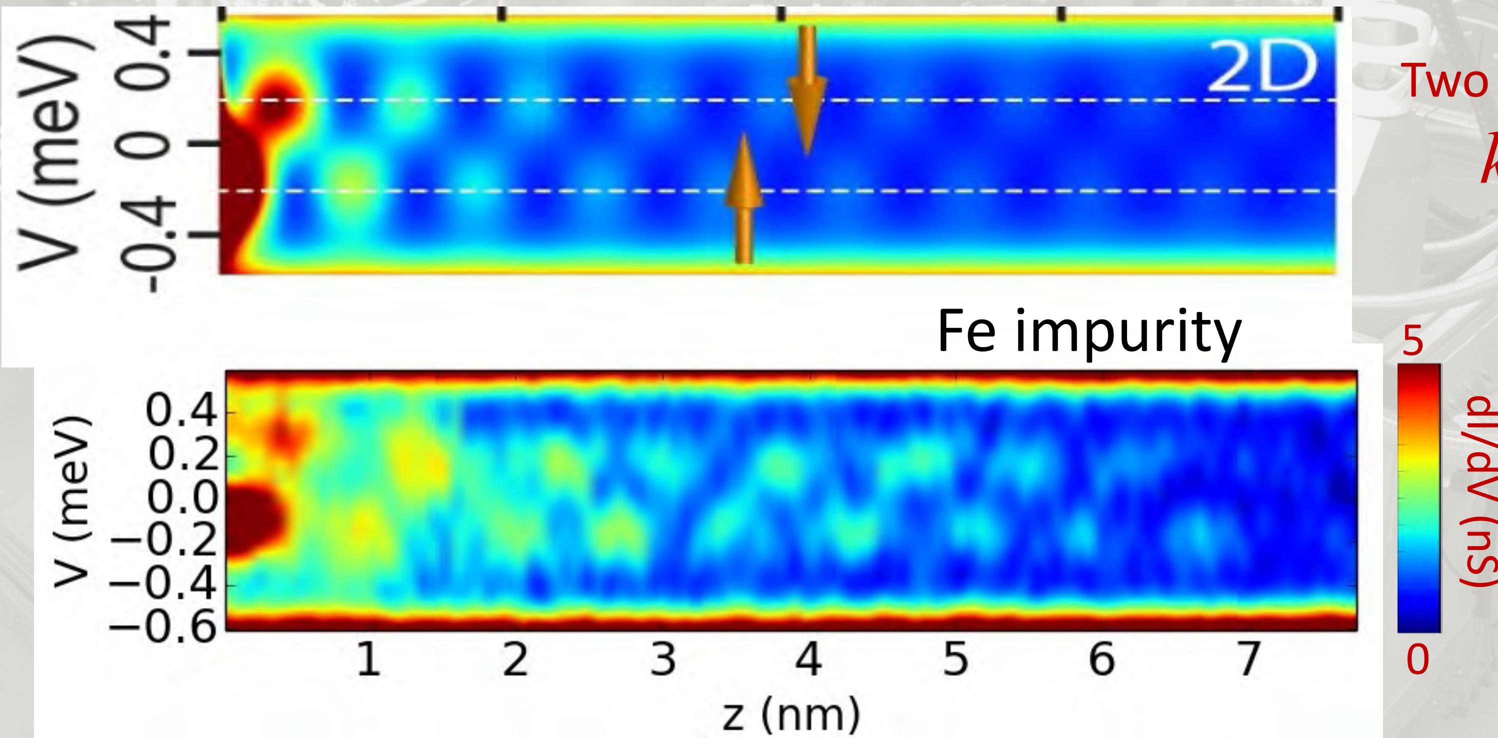

Two char. scales:

k_F and ξ

The phase shift is directly related to the position of the Shiba peaks.

Long-range Shiba bound states – *2H-NbSe$_2$*

$$\psi_{\pm} = \frac{1}{\sqrt{N\pi k_F r}} \sin\left(k_F r - \frac{\pi}{4} + \delta^{\pm}\right) e^{-\sin(\delta^{+}-\delta^{-}) r\Delta/\hbar v_F}$$

$$E_S = \Delta\cos(\delta^{+} - \delta^{-})\,; \quad \tan\delta^{\pm} = K\nu_0 \pm \frac{JS}{2}\nu_0$$

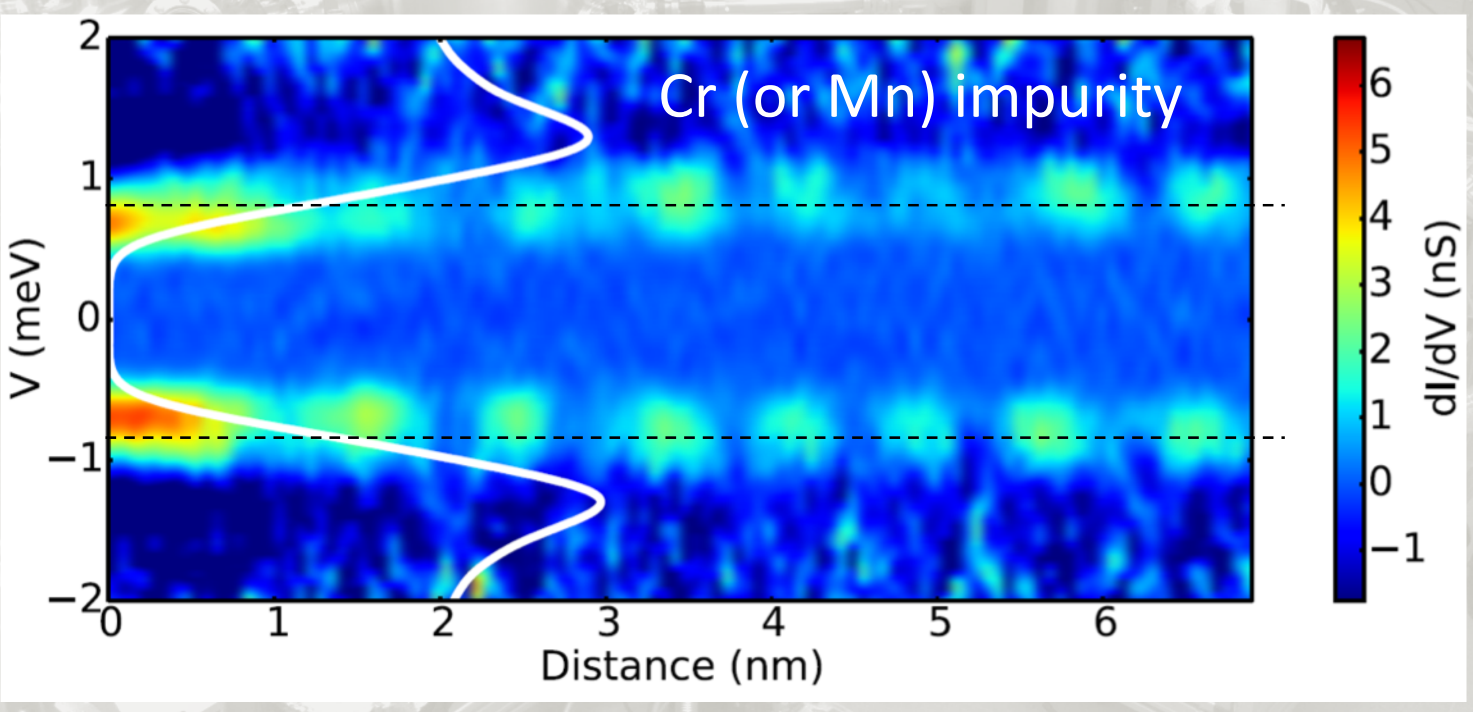

The phase shift is directly related to the position of the Shiba peaks.

Long-range Shiba bound states – *Pb-ML/Si(111)*

$\sqrt{\mathbf{7}}\times\sqrt{\mathbf{3}}$ *Pb*

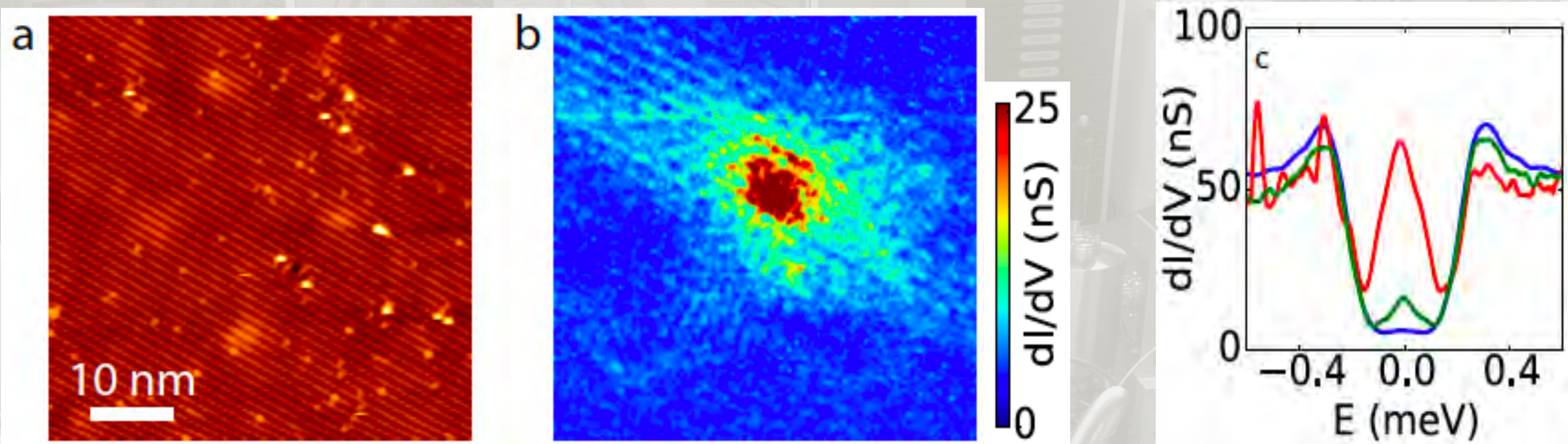

***SIC** Pb*

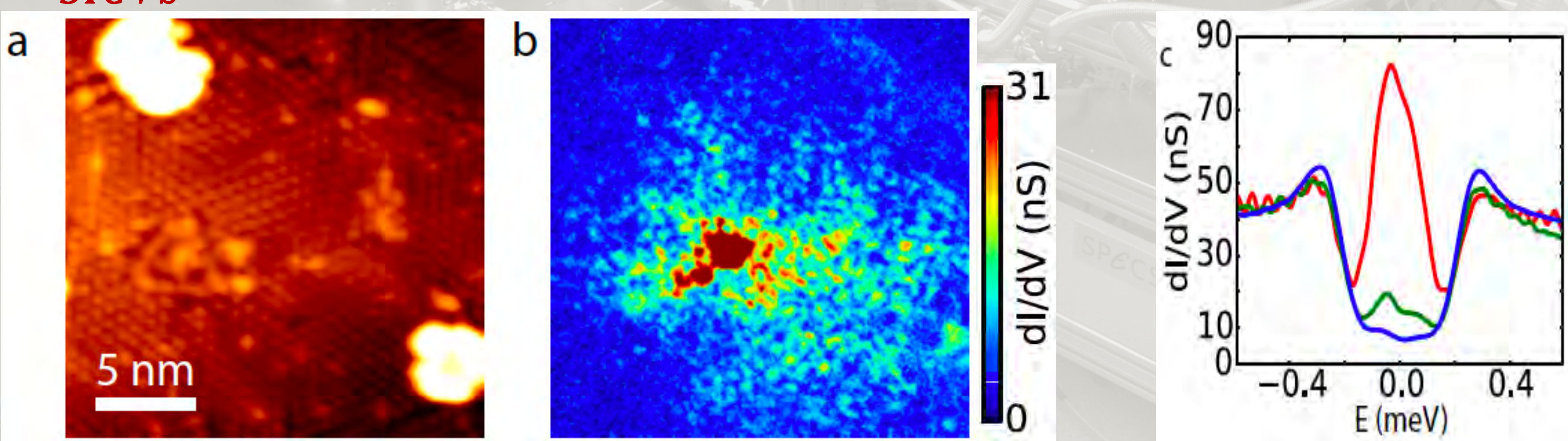

Long-range Shiba bound states

Experimental geometry (coupling, screening):

3D SC, magnetic atoms at the surface

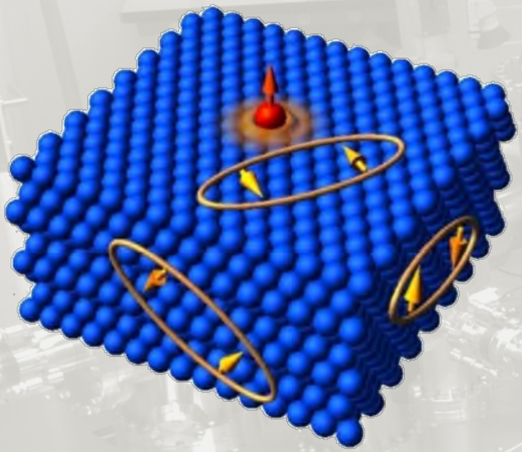

3D

$$\psi_{\pm}(r) = \frac{1}{\sqrt{N}} \frac{\sin\left(k_F r + \delta^{\pm}\right)}{k_F r} e^{-\Delta \sin(\delta^{+}-\delta^{-}) r/\hbar v_F}$$

2D SC, magnetic atoms in the matrix

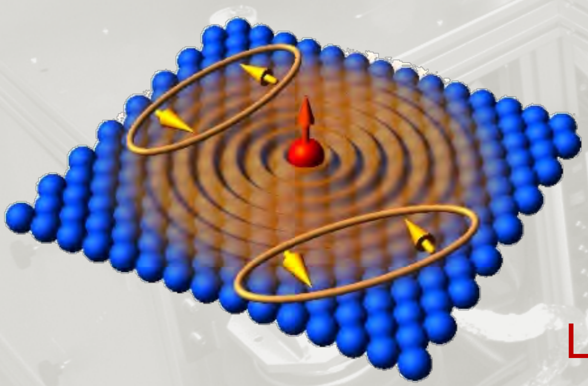

2D

$$\psi_{\pm}(r) = \frac{1}{\sqrt{N\pi}} \frac{\sin\left(k_F r - \frac{\pi}{4} + \delta^{\pm}\right)}{\sqrt{k_F r}} e^{-\Delta \sin(\delta^{+}-\delta^{-}) r/\hbar v_F}$$

Lower dimensionality -> larger extents of YSR bound states

Conclusions 3/4

The relatively long range of the observed Shiba states originates from:

- lower dimensionality (2D or even quasi-1D)
- direct coupling of the imbedded impurity with the SC (instead of a coupling via localized atomic orbitals)

The interference pattern is observed owing clean limit regime

The theoretical description of YSR is confirmed by experimental determination of phase/energy relation

Long range => hope to put several Shiba states in interaction

Outlook

Elementary excitations and vortex in superconducting **Pb-monolayers** *Nat. Phys. (2014)*

Josephson vortex matter in **proximity** junctions *PRL (2013), PRX (2014), Nat. Phys. (2015)*

Long-range Shiba bound states in 2D limit *Nat. Phys. (2015)*

Unconventional **collective** bound states *(2017) to be published*

Unconventional collective bound states

Yet larger concentration of Co-atoms in $\sqrt{7}\times\sqrt{3}$ -Pb/Si(111) –
Formation of Co-islands under Pb

Experiment

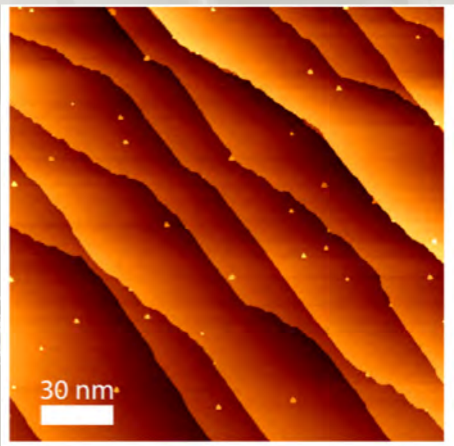

STM

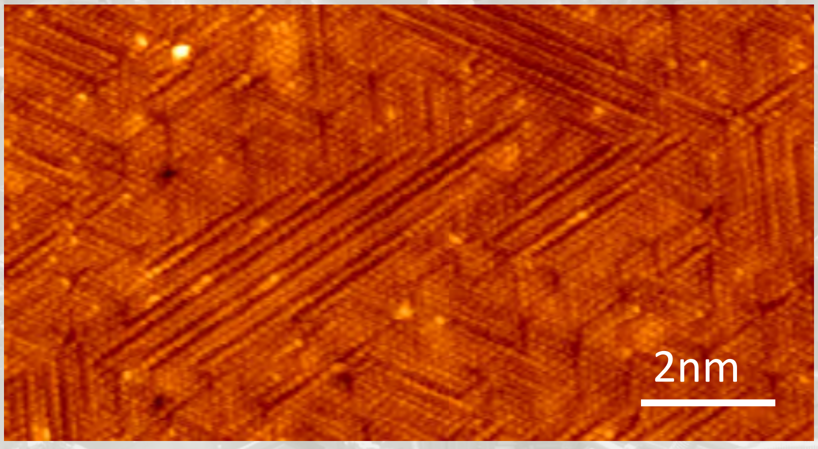

TEM

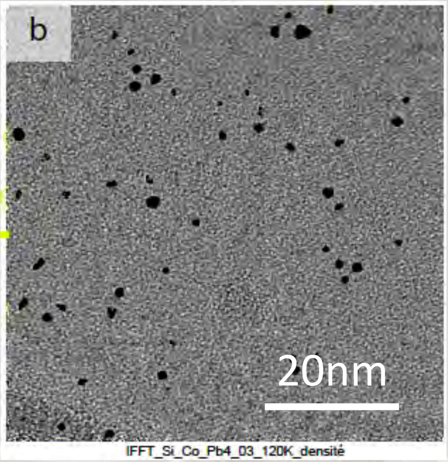

G. Menard et al., arXiv:1607.06353v1 (2016)

Model

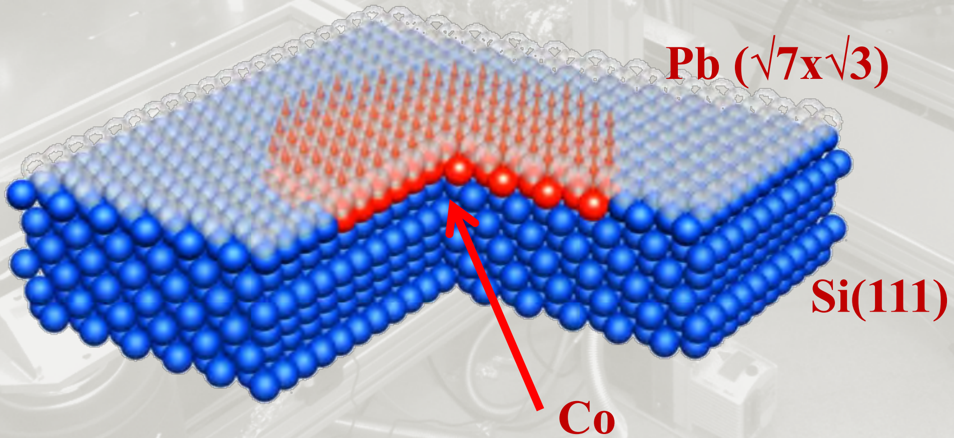

Unconventional collective bound states

Type I states

Individual Co-island under $\sqrt{7}\times\sqrt{3}$ -Pb

STM “topography”

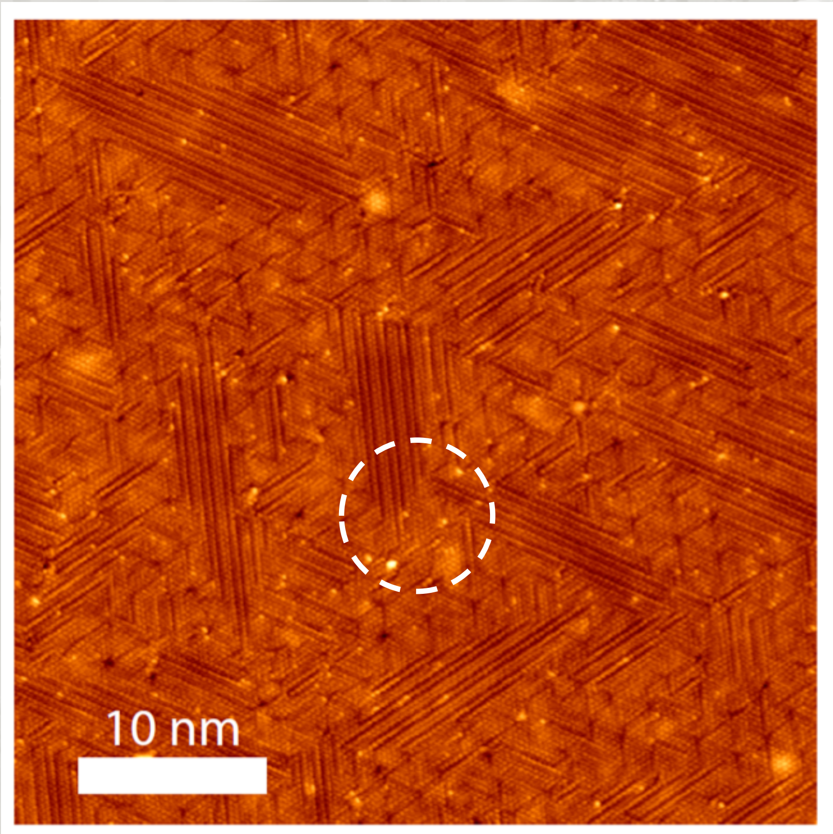

STS zero-bias $dI/dV(x,y)$ map

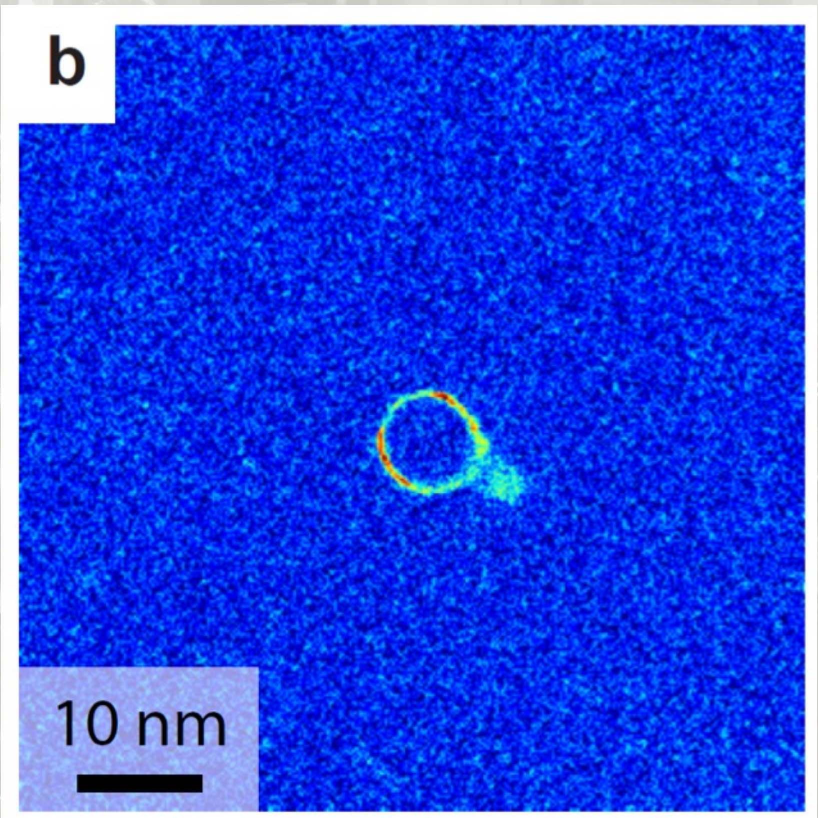

G. Menard et al., arXiv:1607.06353v1 (2016)

Unconventional collective bound states

Type I states

Individual Co-island under $\sqrt{7}\times\sqrt{3}$ -Pb

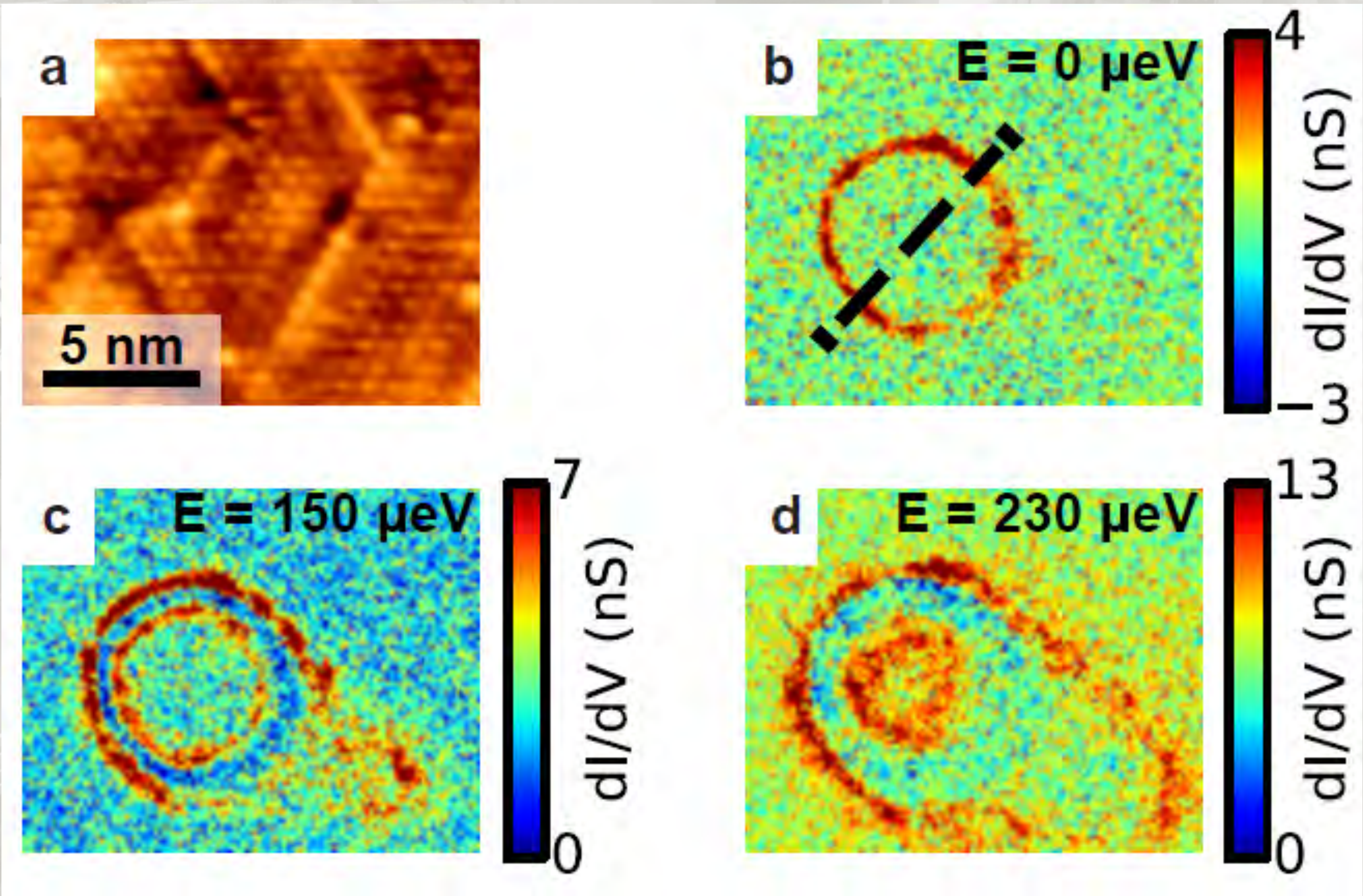

Type I states:

G. Menard et al., arXiv:1607.06353v1 (2016)

Feature 1: No influence of disorder at $V = 0$

Unconventional collective bound states

Type I states

Individual Co-island under $\sqrt{7}\times\sqrt{3}$ -Pb

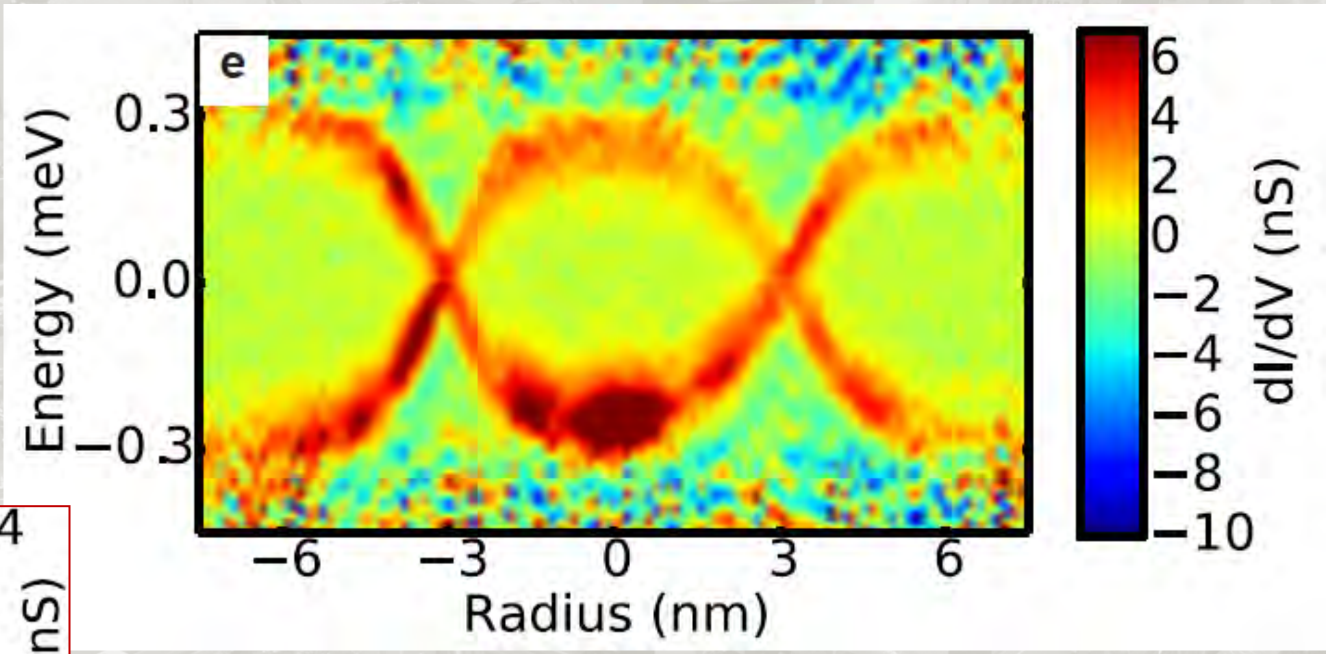

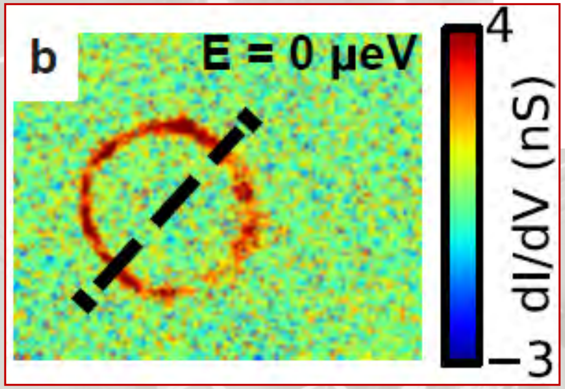

Type I states:

G. Menard et al., arXiv:1607.06353v1 (2016)

Feature 2: Spatial ordering of the Shiba-like state energies (Shiba band)

Conclusions

We observe dispersive in-gap states at the interface between a superconducting domain made of a single atomic layer of Pb covering magnetic islands of Co/Si(111) and the surrounding superconducting $\sqrt{7} \times \sqrt{3}$ – Pb monolayer.

The states demonstrate a surprising spatial protection from the structural disorder. The states at E_F appear perfectly protected.

We speculate the observed continuous dispersion across the superconducting gap to result from a spatial topological transition.

For further details: arXiv:1607.06353v1 (2016)